

Anomalous Diffusion: Fractional Brownian Motion vs. Fractional Ito Motion

Iddo Eliazar* Tal Kachman†

November 12, 2021

Abstract

Generalizing Brownian motion (BM), fractional Brownian motion (FBM) is a paradigmatic selfsimilar model for anomalous diffusion. Specifically, varying its Hurst exponent, FBM spans: sub-diffusion, regular diffusion, and super-diffusion. As BM, also FBM is a symmetric and Gaussian process, with a continuous trajectory, and with a stationary velocity. In contrast to BM, FBM is neither a Markov process nor a martingale, and its velocity is correlated. Based on a recent study of selfsimilar Ito diffusions, we explore an alternative selfsimilar model for anomalous diffusion: *fractional Ito motion* (FIM). The FIM model exhibits the same Hurst-exponent behavior as FBM, and it is also a symmetric process with a continuous trajectory. In sharp contrast to FBM, we show that FIM: is not a Gaussian process; is a Markov process; is a martingale; and its velocity is not stationary and is not correlated. On the one hand, FBM is hard to simulate, its analytic tractability is limited, and it generates only a Gaussian dissipation pattern. On the other hand, FIM is easy to simulate, it is analytically tractable, and it generates non-Gaussian dissipation patterns. Moreover, we show that FIM has an intimate linkage to diffusion in a logarithmic potential. With its compelling properties, FIM offers researchers and practitioners a highly workable analytic model for anomalous diffusion.

Keywords: sub-diffusion; super-diffusion; selfsimilarity; Hurst exponent; non-Gaussian diffusion; diffusion in a logarithmic potential.

PACS: 02.50.-r (probability theory, stochastic processes, and statistics); 05.40.-a (fluctuation phenomena, random processes, noise, and Brownian motion)

*E-mail: eliazar@tauex.tau.ac.il

†Donders Centre for Cognition, Radboud university, Netherlands.

1 Introduction

A recent study [1] characterized the intersection of two principal classes of one-dimensional random motions: the class of selfsimilar processes, and the class of Ito diffusion processes. The former class manifests random motions whose trajectories are, statistically, fractal objects [2]. The latter class manifests random motions whose dynamics are governed by Ito's stochastic differential equation [3]-[5]. Both these classes are of major importance, theoretical and practical alike. In this paper, progressing from the theoretical study [1] to statistical-physics applications, we explore a practical model for *anomalous diffusion*.

Regular and anomalous diffusion assume central roles in science and engineering [6]-[12]. The paradigmatic model for regular diffusion is Brownian motion [13]-[14], which is a mathematical object of exquisite beauty and riches [15]. Maintaining key properties of Brownian motion – namely, being a selfsimilar process with finite variance and with a continuous trajectory – the paradigmatic model for anomalous diffusion is *fractional Brownian motion* [16]-[28]. On the flip side, fractional Brownian motion fails to maintain other key properties of Brownian motion; specifically, fractional Brownian motion is neither a Markov process, nor a martingale [2]. Consequently, both the numerical simulation and the analytic tracking of fractional Brownian motion are challenging tasks.

In analogy with fractional Brownian motion, we term this paper's anomalous-diffusion model *fractional Ito motion*. As fractional Brownian motion, fractional Ito motion also maintains the aforementioned key properties of Brownian motion: it is a selfsimilar process with finite variance and with a continuous trajectory. In sharp contrast to fractional Brownian motion, fractional Ito motion is a Markov process, as well as a martingale. Consequently, fractional Ito motion is a highly useful and a highly workable model for anomalous diffusion.

A Stratonovich counterpart of fractional Ito motion – in which the underpinning Ito integration is replaced by Stratonovich integration – was explored in [29]. A special case of fractional Ito motion was investigated in [30], and, most recently, fractional Ito motion was investigated in the context of stochastic resetting [31]. In this paper, taking on a selfsimilarity approach, we conduct a detailed comparison between two anomalous diffusion models: *fractional Brownian motion* vs. *fractional Ito motion*.

The paper is organized as follows. We begin with an overview of regular and anomalous diffusion, and with a concise description of the three aforementioned models (section 2): Brownian motion, fractional Brownian motion, and fractional Ito motion. We then present the detailed comparison between fractional Brownian motion and fractional Ito motion (section 3). Thereafter, we present a “diffusion-in-a-logarithmic-potential” representation of fractional Ito motion (section 4), and conclude with a summary (section 5).

2 Regular and anomalous diffusion

Diffusion is a generic name for random motions that diffuse with time. Arguably, the most common method to measure diffusivity is mean square displacement (MSD). To describe this method, consider a one-dimensional random motion whose trajectory is $X(t)$ ($t \geq 0$). Namely, the motion initiates at time 0, and its position at time t is $X(t)$ (a point on the real line). Hence, at time t , the motion's displacement – relative to its initial position – is $|X(t) - X(0)|$. In turn, the motion's MSD at time t is $\phi(t) = \mathbf{E}[|X(t) - X(0)|^2]$, where here and hereinafter $\mathbf{E}[\cdot]$ denotes the operation of statistical expectation. Rather generally, the random motion under consideration can be said to be a *diffusion* if: its MSD function $\phi(t)$ increases with time, and diverges as time grows infinitely large.

Often, diffusions take place at microscopic spatio-temporal scales, but yet they are observed at macroscopic spatio-temporal scales. As explained in the Methods, on the macroscopic level the only admissible form of the MSD function is a power-law:

$$\phi(t) = c \cdot t^\epsilon, \quad (1)$$

where c is a positive coefficient, and where ϵ is a positive exponent. A broad and rich framework for random motions that yield such a power-law MSD form are *selfsimilar processes* with finite variance [2]. To describe the notion of selfsimilarity consider, as above, a one-dimensional random motion whose trajectory is $X(t)$ ($t \geq 0$).

The random motion under consideration is selfsimilar if – for any given positive scale s – its two following versions are statistically equal [2]: the time-scaled version $X(st)$ ($t \geq 0$); and the space-scaled version $s^H X(t)$ ($t \geq 0$), where H is a positive *Hurst exponent*. Namely, with regard to the random motion under consideration, selfsimilarity means that: changing the underlying temporal scale from 1 to s is statistically equivalent to changing the underlying spatial scale from 1 to s^H . Selfsimilarity implies that the motion initiates at the spatial origin $X(0) = 0$, and that the random variable $X(t)$ is equal in law to the random variable $t^H \cdot X(1)$. Consequently – in the finite-variance case – selfsimilarity yields the power-law MSD form of Eq. (1) with: coefficient $c = \mathbf{E}[|X(1)|^2]$, and exponent $\epsilon = 2H$.

The above discussion is mathematically neat, yet it is merely theoretical. Does the real world corroborate the theory? The answer is a resounding yes: real-world observations happen to be in perfect accord with the theory. Indeed, pioneered by the experimental observations of Jan Ingen-Housz [32], of Sir Robert Brown [33], and of Jean Perrin [34], a vast body of empirical evidence established the ubiquity of diffusions with linear MSD functions, $\phi(t) = c \cdot t$. Such diffusions are so prevalent that they were assumed to manifest diffusive motions at large. In turn, the convention was to quantify a given diffusive motion by its “diffusion coefficient” – the slope of its linear MSD function.

In the nineteen-seventies of the twentieth century new experimental observations began to challenge the then commonplace assumption that diffusive

motions have linear MSD functions [35]-[39]. As the new body of empirical evidence grew larger and larger, it became clear that in addition to the well-known diffusive motions with linear MSD functions, there are also diffusive motions with power-law MSD functions. Consequently, diffusions were distinguished by three different categories: *regular diffusion*, characterized by linear MSD functions; *sub-diffusion*, characterized by power-law MSD functions with sub-linear exponents $\epsilon < 1$; and *super-diffusion*, characterized by power-law MSD functions with super-linear exponents $\epsilon > 1$.

The experimental discovery of sub-diffusive and super-diffusive random motions ushered in the multidisciplinary scientific field of *anomalous diffusion* [6]-[12]. This field attracted substantial scientific interest [40]-[50], and the scientific exploration of the field led to the conclusions that “anomalous is normal” [51] and that “anomalous is ubiquitous” [52].

Over forty years after its inception, anomalous diffusion continues to be a vibrant multidisciplinary scientific field. Examples of recent anomalous-diffusion research include: anomalous diffusion in complex media [53]; anomalous diffusion in the evolution of inhomogeneous systems [54]; anomalous diffusion in random dynamical systems [55]; anomalous diffusion and recurrent neural networks [56]; heterogeneous diffusion processes [57]; anomalous diffusion in heterogeneous binary media [58]; anomalous diffusion and time-dependent diffusivity [59]; anomalous diffusion in the noisy voter model [60]-[61]; anomalous diffusion under stochastic resetting [62]-[63]; anomalous diffusion in comb structures [64]-[67]; and random diffusivity [68]-[71].

We now turn to describe the three random-motion models that were noted in the introduction. We begin with the paradigmatic models of Brownian motion and fractional Brownian motion. Thereafter, we present the model of fractional Ito motion.

2.1 Brownian motion and fractional Brownian motion

Following the trailblazing theoretical works of Louis Bachelier in finance [72]-[73], of Albert Einstein and Marian Smoluchowski in physics [74]-[75], and of Norbert Wiener in mathematics [76], a particular random motion emerged as the paradigmatic model for regular diffusion in science and engineering [13]-[14]: *Brownian motion* (BM), $B(t)$ ($t \geq 0$). Named in honor of Sir Robert Brown, and also termed *Wiener process* in honor of Norbert Wiener, BM is a profound object that exhibits a host of mathematical, statistical, and geometric properties [15].

In this paper we shall address the following key BM properties. I) BM has finite variance, i.e. its positions have finite first-order and second-order moments; hence BM has a well-defined MSD function. II) BM is a symmetric process, i.e. its trajectory is statistically identical to its mirror trajectory, $-B(t)$ ($t \geq 0$). III) The trajectory of BM is continuous. IV) BM is a selfsimilar process with Hurst exponent $H = \frac{1}{2}$; hence the MSD function of BM is linear, $\epsilon = 1$, and hence it is a regular diffusion indeed. V) BM is a Gaussian process, i.e. its finite-dimensional distributions are multivariate Normal. VI) BM is a Levy

process, i.e. its increments are stationary and its non-overlapping increments are independent. VII) BM is a Markov process, i.e. – at any given time point t – its future trajectory depends only at its present position, $B(t)$, and it does not depend on its past trajectory. VIII) BM is a martingale.

The properties of BM imply that its positions, as well as its increments, are Normal random variables with zero means. The inherent scale of BM is set so that the random variable $B(1)$ – the position of BM at the time point 1 – is “standard Normal”, i.e.: $B(1)$ is a Normal random variable with zero mean and with unit variance.

In order to model anomalous diffusion one needs to go beyond BM. To do so – within the realm of symmetric and selfsimilar processes with finite variance and continuous trajectories – leads to the following model: *fractional Brownian motion* (FBM), $B_H(t)$ ($t \geq 0$), where the subscript H manifests the underlying Hurst exponent. Pioneered by Andrey Kolmogorov [77], by Akiva Yaglom [78], and by Benoit Mandelbrot and John an Ness [79], FBM is a well established generalization of BM [80]-[83]. The Hurst exponent of FBM takes values in the range $0 < H < 1$, and hence the diffusivity of FBM is as follows: sub-diffusion in the exponent range $0 < H < \frac{1}{2}$; super-diffusion in the exponent range $\frac{1}{2} < H < 1$; and regular diffusion at the exponent value $H = \frac{1}{2}$ – in which case FBM is BM.

One the one hand – as BM – FBM is a Gaussian process, its trajectory is continuous, and its increments are stationary [2]. On the other hand – in sharp contrast to BM – the non-overlapping increments of FBM are dependent, and FBM is neither a Markov process nor is it a martingale [2]. Moreover, FBM is not even a semi-martingale, and this fact has major implications in the context of stochastic integration [2].

To gain insight regarding the difference between BM and FBM, we turn to their velocities. The velocity of BM, $\dot{B}(t)$ ($t \geq 0$), is commonly known as *white noise*. The velocity of FBM, $\dot{B}_H(t)$ ($t \geq 0$), is a moving average – with a power-law kernel – of white noise. Specifically, the velocity of FBM with Hurst exponent $H \neq \frac{1}{2}$ admits the following moving-average representation [84]:

$$\dot{B}_H(t) = \left(H - \frac{1}{2}\right) \int_{-\infty}^t (t-u)^{H-\frac{3}{2}} \dot{B}(u) du. \quad (2)$$

The moving-average representation of Eq. (2) actually uses two independent white noises: one defined over the negative time axis, $\dot{B}(u)$ ($u < 0$); and one defined over the non-negative time axis, $\dot{B}(u)$ ($u \geq 0$).

As FBM is a selfsimilar process, it initiates at the spatial origin $B_H(0) = 0$. Hence, integrating Eq. (2) yields

$$B_H(t) = \int_{-\infty}^0 \left[(t-u)^{H-\frac{1}{2}} - (0-u)^{H-\frac{1}{2}}\right] \dot{B}(u) du + \int_0^t (t-u)^{H-\frac{1}{2}} \dot{B}(u) du. \quad (3)$$

The integral representation of Eq. (3) comprises two parts: an integral of the white noise $\dot{B}(u)$ over the negative temporal axis, $-\infty < u < 0$; and an integral

of the white noise $\dot{B}(u)$ over the temporal interval $0 \leq u \leq t$. The integral representation of Eq. (3) covers also the Hurst exponent $H = \frac{1}{2}$, and setting this Hurst exponent in Eq. (3) yields BM: $B_{1/2}(t) = B(t)$. Hence, FBM is indeed a generalization of BM. Schematic illustrations of the integration kernel of Eq. (3) – whose shape is determined by the value of the Hurst exponent H – are depicted in Figure 1.

As noted above, FBM is not a Markov process. There are one-dimensional random motions that are non-Markov, but yet they can be transformed to a Markov-process representation by elevating from a single dimension to several dimensions. FBM is a highly non-Markov process in the following sense: in order to transform FBM to a Markov-process representation one has to elevate from a single dimension to infinitely many dimensions [84]. Consequently, the numerical simulation of FBM is a challenging computational task [85]-[94].

So, on the one hand, FBM is a random-motion model – which is selfsimilar and Gaussian, whose positions have a finite variance, and whose trajectory is continuous – that produces both sub-diffusion and super-diffusion. On the other hand, working with FBM is quite challenging from the perspectives of stochastic integration and numerical simulation, as well as from the perspective of analytic tractability. The intricacy of FBM gives rise to the following question: is there an alternative anomalous-diffusion model that shares the ‘upside’ features of FBM, but not the ‘downside’ features of FBM? The answer, as we shall now argue, is affirmative indeed.

2.2 Fractional Ito motion

Consider a one-dimensional deterministic motion $X(t)$ ($t \geq 0$), whose dynamics are governed by the ordinary differential equation (ODE) $\dot{X}(t) = \mu[X(t)]$. Namely, when the deterministic motion is at the position x (a point on the real line) then its velocity is $\mu(x)$ (a real number). Adding white noise to the dynamics changes the motion from deterministic to random, and changes the ODE to a Langevin stochastic differential equation (SDE) [95]-[97]: $\dot{X}(t) = \mu[X(t)] + \nu\dot{B}(t)$, where ν is a positive parameter that manifest the white-noise magnitude. In turn, replacing the constant white-noise magnitude ν by a position-dependent magnitude changes the Langevin SDE to an Ito SDE [3]-[5],[98]-[99]: $\dot{X}(t) = \mu[X(t)] + \sigma[X(t)]\dot{B}(t)$. In the jargon of mathematical finance [100]: when the random motion is at the position x (a point on the real line) then its “drift” is $\mu(x)$ (a real number), and its “volatility” is $\sigma(x)$ (a positive number).

With the notion of Ito SDEs recalled, we introduce the following model: *fractional Ito motion* (FIM), $I_H(t)$ ($t \geq 0$), where the subscript H manifests the underlying Hurst exponent. In analogy with FBM, we name FIM in honor of Kioshi Ito – the mathematician that invented the white-noise stochastic calculus. The dynamics of FIM are governed by the Ito SDE

$$\dot{I}_H(t) = |I_H(t)|^{1-\frac{1}{2H}} \dot{B}(t) \quad (4)$$

Namely, FIM has a zero drift, $\mu(x) = 0$, and a power-law volatility, $\sigma(x) = |x|^{1-\frac{1}{2H}}$. In general, a random motion whose dynamics are governed by an Ito SDE is a Markov process, and its trajectory is continuous [15]; hence, in particular, FIM exhibits these properties.

We initiate FIM from the spatial origin $I_H(0) = 0$. Hence, integrating Eq. (4) yields

$$I_H(t) = \int_0^t |I_H(u)|^{1-\frac{1}{2H}} \dot{B}(u) du. \quad (5)$$

The right-hand side of Eq. (5) is a running Ito integral. A general running Ito integral – with an integrand that does not ‘look into the future’ – is a symmetric process and a martingale [15]; hence, in particular, FIM exhibits these properties.

According to general results regarding selfsimilar diffusions [1], FIM is a selfsimilar process, and the Hurst exponent of FIM takes values in the range $0 < H < 1$. Hence, the diffusivity of FIM is identical to the aforementioned diffusivity of FBM: sub-diffusion in the exponent range $0 < H < \frac{1}{2}$; super-diffusion in the exponent range $\frac{1}{2} < H < 1$; and regular diffusion at the exponent value $H = \frac{1}{2}$ – in which case FIM is BM. Indeed, setting $H = \frac{1}{2}$ in Eq. (5) yields BM: $I_{1/2}(t) = B(t)$. Schematic illustrations of the FIM ‘volatility landscape’ – whose shape is determined by the value of the Hurst exponent H – are depicted in Figure 1.

So, on the one hand, FIM shares the ‘upside’ features of FBM: it is a random-motion model – which is symmetric and selfsimilar, and whose trajectory is continuous – that generalizes BM, and that produces both sub-diffusion and super-diffusion. On the other hand, as FIM is a Markov process and a martingale, it circumvents the ‘downside’ features of FBM: it well applies in the context of stochastic integration, its numerical simulation is easy and straightforward, and it is analytically tractable.

Replacing the Ito SDE (4) by an identical Stratonovich SDE results in a “fractional Stratonovich motion” counterpart of FIM; this counterpart of the FIM model was explored in [29]. A special case of the FIM model was investigated in [30]; in this special case the motion runs over the positive half-line ($0 < x < \infty$), and the Hurst exponent is in the range $\frac{1}{2} \leq H < 1$. Most recently, FIM was also investigated in the context of stochastic resetting [31]. To the best of our knowledge, the detailed FBM vs. FIM comparison – which is conducted and presented in this paper – is entirely new.

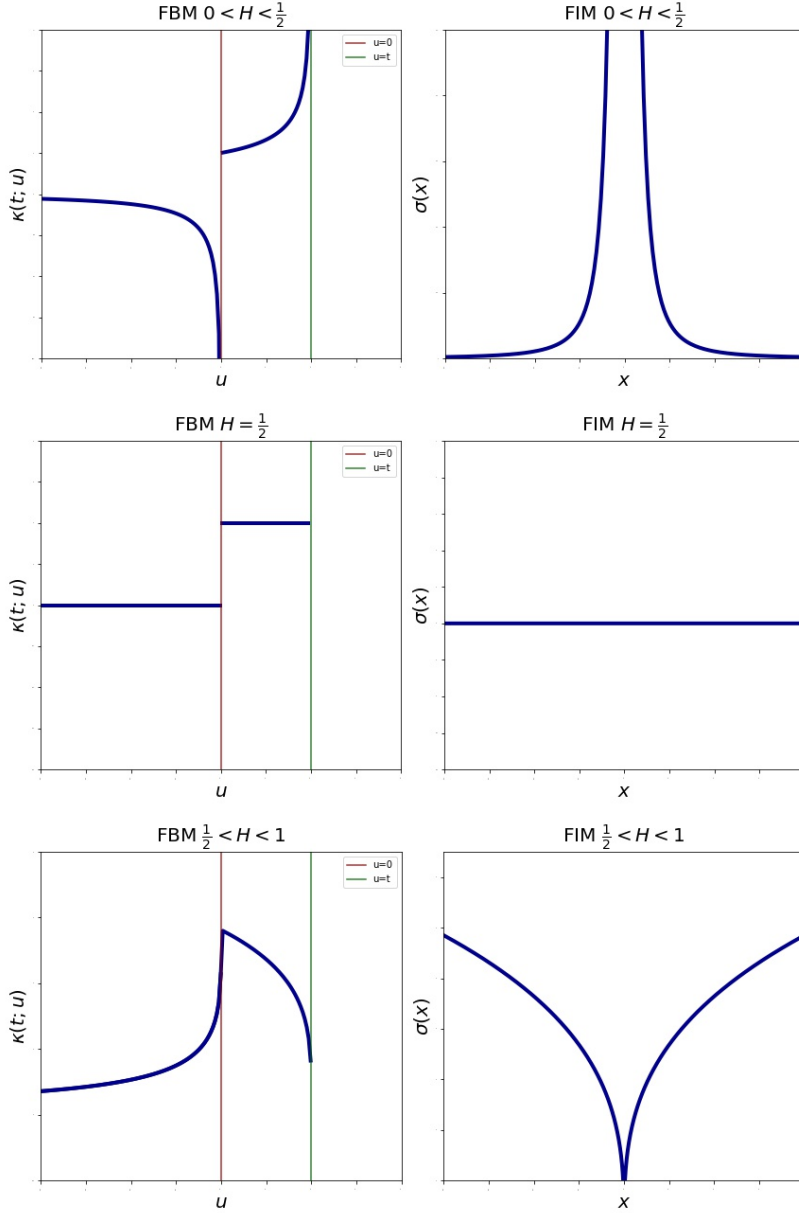


Figure 1: schematic illustrations of the shapes of the FBM integration kernel, and of the FIM volatility landscape. Depicted in the left panels, the FBM integration kernel (for a fixed positive time point t) is: $\kappa(t; u) = (t - u)^{H - \frac{1}{2}} - (0 - u)^{H - \frac{1}{2}}$ over the negative temporal axis, $-\infty < u < 0$; and $\kappa(t; u) = (t - u)^{H - \frac{1}{2}}$ over the temporal interval $0 \leq u \leq t$. Depicted in the right panels, the FIM volatility landscape is: $\sigma(x) = |x|^{1 - \frac{1}{2H}}$ over the spatial axis $-\infty < x < \infty$. The temporal kernel function $\kappa(t; u)$ and the spatial volatility function $\sigma(x)$ display markedly different shapes in the three different diffusivity categories: sub-diffusion $0 < H < \frac{1}{2}$ (top panels); super-diffusion $\frac{1}{2} < H < 1$ (bottom panels); and regular diffusion $H = \frac{1}{2}$ (middle panels).

3 Fractional Brownian motion vs. fractional Ito motion

Describing the FBM model and FIM model, the previous section revealed some of the marked differences between these two anomalous-diffusion models. In this section we carry on with a series of analytic comparisons that examine and pinpoint additional profound differences between FBM and FIM. Visual comparisons between simulated trajectories of FBM and FIM are offered by Figure 2 (for sub-diffusion) and by Figure 3 (for super-diffusion).

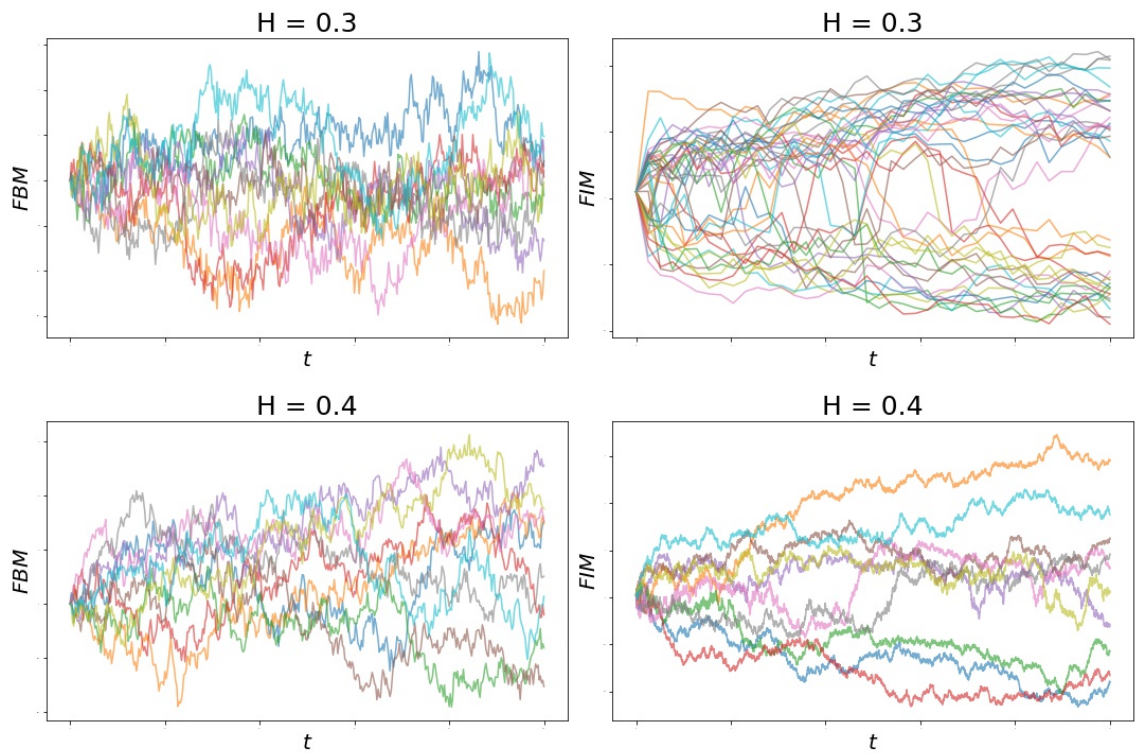


Figure 2: simulated trajectories of sub-diffusive FBM (left panels) and of sub-diffusive FIM (right panels).

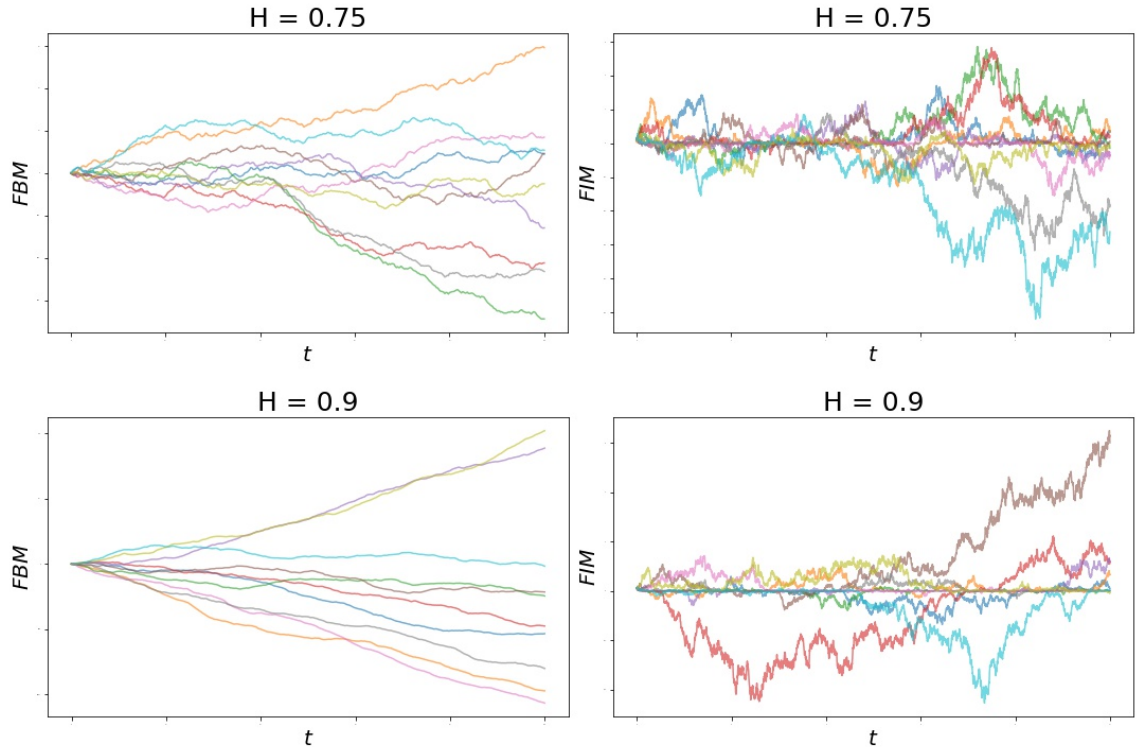


Figure 3: simulated trajectories of super-diffusive FBM (left panels) and of super-diffusive FIM (right panels).

3.1 Dissipation comparison

As FBM and FIM are selfsimilar processes, they both initiate from the spatial origin. Hence, from a probabilistic perspective, at time 0 both these random motions manifest a unit mass that is placed at the origin. In turn, at a positive time t , this unit mass dissipates, and the ‘shape of the dissipation’ is quantified by a probability density function: the density of the random variable $B_H(t)$, in the case of FBM; and the density of the random variable $I_H(t)$, in the case of FIM.

The properties of FBM imply that the random variable $B_H(t)$ is Normal with mean zero with variance $\mathbf{Var}[B_H(t)] = \mathbf{Var}[B_H(1)] \cdot t^{2H}$. Hence, setting $b = \mathbf{Var}[B_H(1)]$, the density of the random variable $B_H(t)$ is

$$\frac{1}{\sqrt{2\pi b}} \cdot \frac{1}{t^H} \exp\left(-\frac{x^2}{2bt^{2H}}\right) \quad (6)$$

($-\infty < x < \infty$). This density is a symmetric ‘bell curve’ (see Figure 4): it vanishes at $x \rightarrow \pm\infty$, and it has a unimodal shape the peaks at the spatial

origin. We emphasize that the shape of this density is the same for all the values of the Hurst exponent H .

It follows from a general result established in [1] that the density of the random variable $I_H(t)$ is

$$\frac{1}{2H\Gamma(1-H)} \cdot \left(\frac{2H^2}{t}\right)^{1-H} \exp\left(-\frac{2H^2}{t} |x|^{\frac{1}{H}}\right) |x|^{\frac{1}{H}-2} \quad (7)$$

($-\infty < x < \infty$). This density is symmetric, and it vanishes at $x \rightarrow \pm\infty$. The shape of this density is determined by the value of the Hurst exponent H , as follows (see Figure 4).

- In the sub-diffusion range, $0 < H < \frac{1}{2}$, the density has a bimodal shape: it vanishes at the spatial origin, and it peaks at the spatial points $\pm \left(\frac{1-2H}{2H^2}\right) t^H$.
- At the regular-diffusion value, $H = \frac{1}{2}$, the density is a ‘bell curve’: it has a unimodal shape the peaks at the spatial origin.
- In the super-diffusion range, $\frac{1}{2} < H < 1$, the density has a unimodal shape the explodes at the spatial origin.

Evidently, the differences between the shape of the Gaussian FBM density of Eq. (6) and the shape of the non-Gaussian (for $H \neq \frac{1}{2}$) FIM density of Eq. (7) are dramatic. On the one hand, changing the Hurst exponent H in the FBM model has no qualitative effect on the shape of the dissipation pattern. On the other hand, changing the Hurst exponent H in the FIM model has a profound qualitative effect on the shape of the dissipation pattern.

The dissipation pattern of “fractional Stratonovich motion” – the Stratonovich counterpart of FIM – displays a behavior which is similar to that of the FIM density of Eq. (7) [29]. Non-Gaussian diffusions (i.e. diffusions with non-Gaussian dissipation patterns), such as FIM and its Stratonovich counterpart, attracted substantial scientific interest recently [101]-[109].

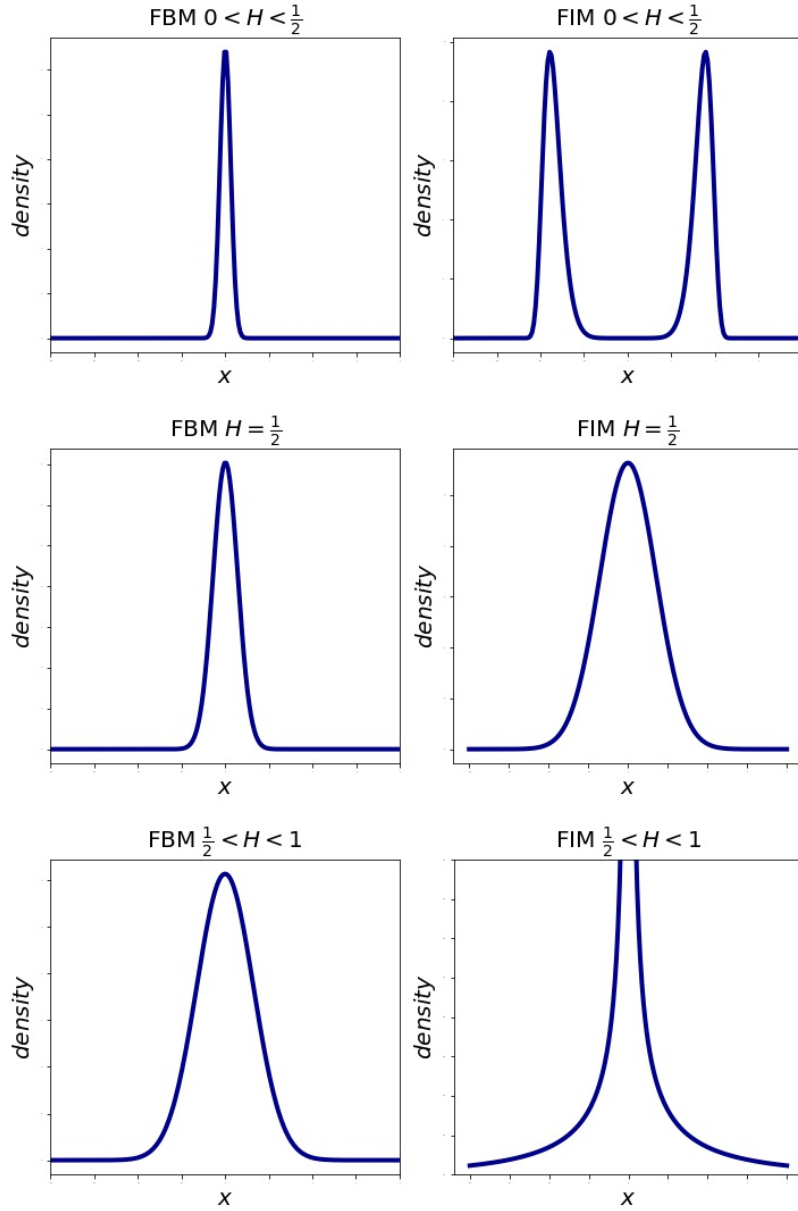


Figure 4: schematic illustrations of the shapes of the FBM and FIM dissipation patterns (for a fixed positive time point t). Depicted in the left panels, the FBM dissipation pattern is the probability density function of the random variable $B_H(t)$ (Eq. (6)). Depicted in the right panels, the FIM dissipation pattern is the probability density function of the random variable $I_H(t)$ (Eq. (7)). While the FBM dissipation pattern displays the same unimodal ‘bell-curve’ shape, the FIM dissipation pattern displays markedly different shapes in the three different diffusivity categories: bimodal for sub-diffusion $0 < H < \frac{1}{2}$ (top panels); unimodal and explosive for super-diffusion $\frac{1}{2} < H < 1$ (bottom panels); and unimodal ‘bell-curve’ for regular diffusion $H = \frac{1}{2}$ (middle panels).

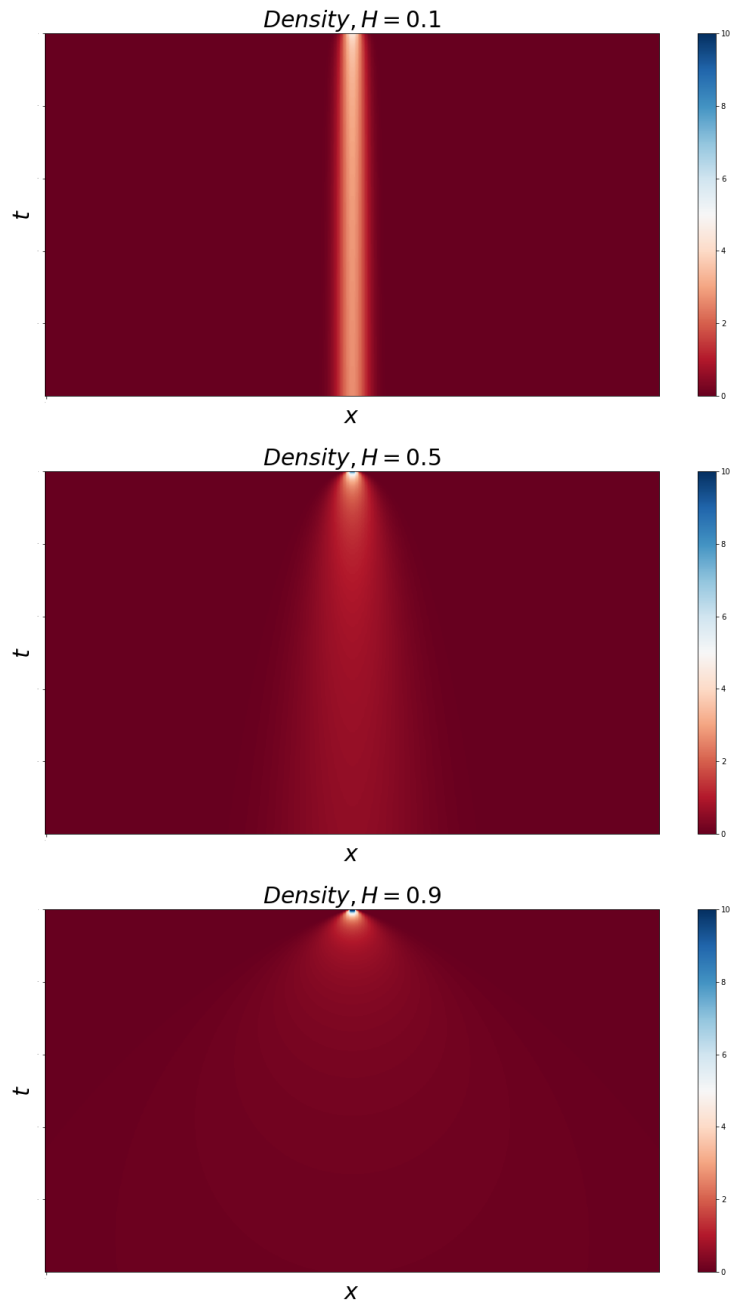


Figure 5: ‘heat maps’ for three examples of the FBM dissipation pattern – the probability density function of the random variable $B_H(t)$ (Eq. (6)). The examples correspond to the three different diffusivity categories of FBM: sub-diffusion (top panel); regular diffusion (middle panel); super diffusion (bottom panel).

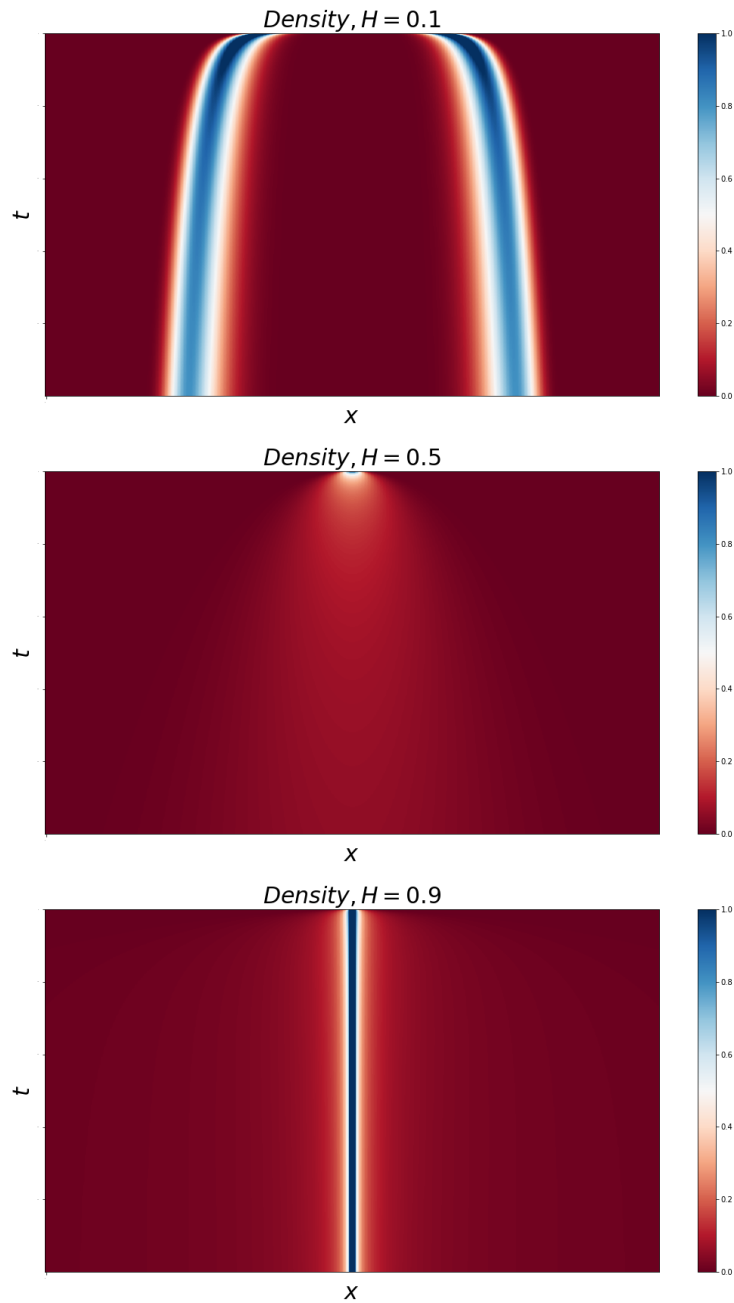


Figure 6: ‘heat maps’ for three examples of the FIM dissipation pattern – the probability density function of the random variable $I_H(t)$ (Eq. (7)). The examples correspond to the three different diffusivity categories of FIM: sub-diffusion (top panel); regular diffusion (middle panel); super diffusion (bottom panel).

3.2 Tail-behavior comparison

Consider a symmetric one-dimensional random motion whose trajectory is $X(t)$ ($t \geq 0$). The tail behavior of the random motion under consideration is the asymptotic behavior of the probability $\Pr[|X(t)| > l]$ in the limit $l \rightarrow \infty$. Namely, the tail behavior quantifies the asymptotic likelihood of the following rare event: the motion’s displacement, at time t , relative to its initial position, is greater than the level $l \gg 1$.

Using Eqs. (6)-(7) and L’Hospital’s rule, we conduct three tail-behavior comparisons: FBM vs. BM; FIM vs. BM; and FIM vs. FBM. These tail-behavior comparisons are presented in Table 1, and they yield the following ‘asymptotic orderings’. In the case of sub-diffusion ($0 < H < \frac{1}{2}$): the tail behavior of FIM is infinitely ‘lighter’ than the tail behavior of FBM – which, in turn, is infinitely ‘lighter’ than the tail behavior of BM. In the case of super-diffusion ($\frac{1}{2} < H < 1$): the tail behavior of FIM is infinitely ‘heavier’ than the tail behavior of FBM – which, in turn, is infinitely ‘heavier’ than the tail behavior of BM.

Table 1

Comparison	Limit	Sub diffusion ($0 < H < \frac{1}{2}$)	Super diffusion ($\frac{1}{2} < H < 1$)
1) FBM vs. BM	$\lim_{l \rightarrow \infty} \frac{\Pr[B_H(t) > l]}{\Pr[B(t) > l]} =$	0	∞
2) FIM vs. BM	$\lim_{l \rightarrow \infty} \frac{\Pr[I_H(t) > l]}{\Pr[B(t) > l]} =$	0	∞
3) FIM vs. FBM	$\lim_{l \rightarrow \infty} \frac{\Pr[I_H(t) > l]}{\Pr[B_H(t) > l]} =$	0	∞

Table 1: tail-behavior comparisons. The comparisons are specified with regard to the two anomalous-diffusion categories: sub-diffusion, ($0 < H < \frac{1}{2}$); and super-diffusion ($\frac{1}{2} < H < 1$). For sub-diffusion: the tail behavior of FIM is infinitely ‘lighter’ than the tail behavior of FBM – which, in turn, is infinitely ‘lighter’ than the tail behavior of BM. Conversely, for super-diffusion: the tail behavior of FIM is infinitely ‘heavier’ than the tail behavior of FBM – which, in turn, is infinitely ‘heavier’ than the tail behavior of BM.

3.3 Statistical-heterogeneity comparison

Inequality indices are quantitative gauges that – using a socioeconomic-inequality perspective – score the statistical heterogeneity of non-negative random variables with positive means [110]-[112]. We shall now use a particular inequality

index in order to compare the inherent statistical heterogeneity of FBM to the inherent statistical heterogeneity of FIM.

Inequality indices are widely applied in economics and in the social sciences to measure wealth inequalities in human societies [113]-[116]. An inequality index takes values in the unit interval, and with regard to a human society under consideration: the lower the inequality-index score – the more egalitarian the distribution of wealth among the society members; and the higher the inequality-index score – the less egalitarian the distribution of wealth among the society members. In particular, the inequality index yields a zero score only when the society under consideration is communist – in which case all the society members share a common (positive) wealth value. Inequality indices are invariant with respect to the specific currency via which wealth is measured (e.g. Dollar or Euro).

Given an inequality index \mathcal{I} , and given a non-negative random variable W with a positive mean, the statistical heterogeneity of the random variable can be measured by the inequality index as follows [112]: deem the random variable W to manifest the personal wealth value of a member that is sampled at random from a virtual human society; then, set the statistical-heterogeneity score of the random variable W to be the inequality-index score of the virtual human society. In what follows we denote by $\mathcal{I}(W)$ the statistical-heterogeneity score that the inequality index \mathcal{I} assigns to the random variable W .

As \mathcal{I} is an inequality index, the score $\mathcal{I}(W)$ exhibits the two following properties. **I**) It takes values in the unit interval, $0 \leq \mathcal{I}(W) \leq 1$, and it vanishes if and only if the random variable is deterministic: $\mathcal{I}(W) = 0 \Leftrightarrow W = \text{const}$ (with probability one). **II**) It is invariant with respect to changes of scale of the random variable: $\mathcal{I}(s \cdot W) = \mathcal{I}(W)$, where s is any positive scale.

The particular inequality index \mathcal{I} that we shall use is based on the first-order and second-order moments of the random variable W , and its statistical-heterogeneity score is [112],[117]: $\mathcal{I}(W) = 1 - \mathbf{E}[W]^2 / \mathbf{E}[W^2]$. This statistical-heterogeneity score is unique in the following sense: it is the only score that has a one-to-one correspondence with the coefficient of variation (CV) of the random variable W , i.e. the ratio of the random-variable's standard deviation to the random-variable's mean. In short, we henceforth term this statistical-heterogeneity score "CV score".

Consider a selfsimilar one-dimensional random motion whose trajectory is $X(t)$ ($t \geq 0$), and whose Hurst exponent is H . We set the focus on the random variable $|X(t)|$ – the motion's displacement, at time t , relative to its initial position. The motion's selfsimilarity implies that the random variable $|X(t)|$ is equal in law to the random variable $t^H \cdot |X(1)|$. In turn, assuming that the random variable $|X(1)|$ has a positive mean, the scaling property of inequality indices implies that: $\mathcal{I}(|X(t)|) = \mathcal{I}(|X(1)|)$. Hence, the quantity $\mathcal{I}(|X(1)|)$ is, in effect, a statistical-heterogeneity score of the selfsimilar random motion under consideration.

In the case of FBM the random variable $B_H(1)$ is a Normal random variable with zero mean. In turn, a probabilistic calculation that is detailed in the

Methods asserts that the CV score of FBM is

$$\mathcal{I} [|B_H(1)|] = 1 - \frac{2}{\pi} . \quad (8)$$

This CV score does not depend on the value of the Hurst exponent H .

In the case of FIM the statistical distribution of the random variable $I_H(1)$ is governed by the density function of Eq. (7). In turn, a probabilistic calculation that is detailed in the Methods asserts that the CV score of FIM is

$$\mathcal{I} [|I_H(1)|] = 1 - \frac{\sin(\pi H)}{\pi H} . \quad (9)$$

This CV score depends on the value of the Hurst exponent H , and as a function of the Hurst exponent $0 < H < 1$ (see Figure 7): it increases from the zero lower-bound score $\lim_{H \rightarrow 0} \mathcal{I} [|I_H(1)|] = 0$ to the unit upper-bound score $\lim_{H \rightarrow 1} \mathcal{I} [|I_H(1)|] = 1$.

Evidently, the difference between the CV score of Eq. (8) and the CV score of Eq. (9) is dramatic. On the one hand, changing the Hurst exponent H in the FBM model has no effect on the inherent statistical heterogeneity. On the other hand, changing the Hurst exponent H in the FIM model has a profound effect on the inherent statistical heterogeneity – which spans the full unit-interval range of statistical-heterogeneity scores.

3.4 Divergence comparison

Consider a selfsimilar one-dimensional random motion whose trajectory is $X(t)$ ($t \geq 0$), and whose Hurst exponent is H . As noted above, the motion’s self-similarity implies that the random variable $X(t)$ is equal in law to the random variable $t^H \cdot X(1)$. Hence, the random variable $X(1)$ – the motion’s position at the time point 1 – is a ‘benchmark’ for the motion’s positions at all times.

In the previous subsection we focused on quantifying the inherent statistical heterogeneity of the random variable $|X(t)|$ – the motion’s displacement, at time t , relative to its initial position. In this subsection we shall focus on quantifying the statistical divergence of the random variable $X(t)$ from its benchmark – the random variable $X(1)$. To that end we use the Kulback-Leibler (KL) divergence [118]-[119], which is arguably the most widely applied measure of statistical divergence. Specifically, the KL divergence of the random variable $X(t)$ from its benchmark $X(1)$ is: $\mathcal{D} [X(t) || X(1)] = \int_{-\infty}^{\infty} \ln [f_t(x) / f_1(x)] f_t(x) dx$, where $f_t(x)$ is the density of the random variable $X(t)$ (and, in particular, $f_1(x)$ is the density of the benchmark $X(1)$).

With regard to FBM, a probabilistic calculation that is detailed in the Methods asserts that the KL divergence of the position $B_H(t)$ from the benchmark position $B_H(1)$ is

$$\mathcal{D} [B_H(t) || B_H(1)] = \frac{1}{2} (t^{2H} - 1) - H \ln(t) . \quad (10)$$

The asymptotic behavior of this KL divergence, in the temporal limit $t \rightarrow \infty$, is $\mathcal{D} [B_H(t) || B_H(1)] \approx \frac{1}{2} t^{2H}$.

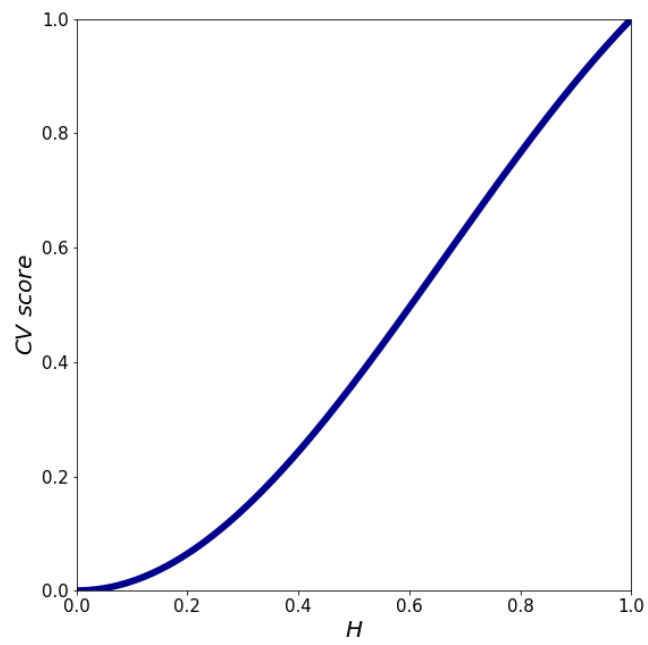


Figure 7: the FIM CV score of Eq. (9), as a function of the Hurst exponent $0 < H < 1$. Varying the value of the Hurst exponent, the full unit-interval range of the CV score is attained.

With regard to FIM, a probabilistic calculation that is detailed in the Methods asserts that the KL divergence of the position $I_H(t)$ from the benchmark position $I_H(1)$ is

$$\mathcal{D}[I_H(t) || I_H(1)] = (1 - H) [t - 1 - \ln(t)] . \quad (11)$$

The asymptotic behavior of this KL divergence, in the temporal limit $t \rightarrow \infty$, is $\mathcal{D}[I_H(t) || I_H(1)] \approx (1 - H) t$.

As a function of the temporal variable t , the KL divergences of Eqs. (10) and (11) share, qualitatively, a common U shape with: a unique global minimum – whose value is zero – that is attained at the time point 1. However, quantitatively, these KL divergences yield dramatically different asymptotic behaviors. Using these asymptotic behaviors, we conduct three divergence comparisons: FBM vs. BM; FIM vs. BM; and FIM vs. FBM. These divergence comparisons are presented in Table 2, and they yield the following ‘asymptotic orderings’. In the case of sub-diffusion ($0 < H < \frac{1}{2}$): the FIM asymptotics are equivalent to the BM asymptotics – which, in turn, are infinitely ‘lighter’ than the FBM asymptotics. In the case of super-diffusion ($\frac{1}{2} < H < 1$): the FIM asymptotics are equivalent to the BM asymptotics – which, in turn, are infinitely ‘heavier’ than the FBM asymptotics.

Table 2

Comparison	Limit	Sub diffusion ($0 < H < \frac{1}{2}$)	Super diffusion ($\frac{1}{2} < H < 1$)
1) FBM vs. BM	$\lim_{t \rightarrow \infty} \frac{\mathcal{D}[B_H(t) B_H(1)]}{\mathcal{D}[B(t) B(1)]} =$	0	∞
2) FIM vs. BM	$\lim_{t \rightarrow \infty} \frac{\mathcal{D}[I_H(t) I_H(1)]}{\mathcal{D}[B(t) B(1)]} =$	$2(1 - H)$	
3) FIM vs. FBM	$\lim_{t \rightarrow \infty} \frac{\mathcal{D}[I_H(t) I_H(1)]}{\mathcal{D}[B_H(t) B_H(1)]} =$	0	∞

Table 2: asymptotic KL-divergence comparisons. The comparisons are specified with regard to the two anomalous-diffusion categories: sub-diffusion ($0 < H < \frac{1}{2}$); and super-diffusion ($\frac{1}{2} < H < 1$). For sub-diffusion: the FIM asymptotics – which are equivalent to the BM asymptotics – are infinitely ‘lighter’ than the FBM asymptotics. Conversely, for super-diffusion: the FIM asymptotics – which are equivalent to the BM asymptotics – are infinitely ‘heavier’ than the FBM asymptotics.

3.5 Aging comparison

Consider a symmetric one-dimensional random motion whose trajectory is $X(t)$ ($t \geq 0$). The motion's displacement over the temporal interval $[t, t + \Delta]$ – where Δ is the interval's positive length – is $|X(t + \Delta) - X(t)|$. In turn, the motion's mean square displacement (MSD) over the temporal interval $[t, t + \Delta]$ is $\mathbf{E}[|X(t + \Delta) - X(t)|^2]$. And, as the motion is symmetric, this MSD is equal to $\mathbf{Var}[X(t + \Delta) - X(t)]$ – the variance of the increment $X(t + \Delta) - X(t)$. In this subsection we shall compare the variance of the FBM increment $B_H(t + \Delta) - B_H(t)$ to the variance of the FIM increment $I_H(t + \Delta) - I_H(t)$.

As FBM initiates at the spatial origin, and as the increments of FBM are stationary, the FBM increment $B_H(t + \Delta) - B_H(t)$ is equal in law to the random variable $B_H(\Delta)$. In turn, as FBM is a selfsimilar process with Hurst exponent H , the random variable $B_H(\Delta)$ is equal in law to the random variable $\Delta^H \cdot B_H(1)$. Consequently, the FBM increment $B_H(t + \Delta) - B_H(t)$ is a Normal random variable with mean zero and with variance

$$\mathbf{Var}[B_H(t + \Delta) - B_H(t)] = \mathbf{Var}[B_H(1)] \cdot \Delta^{2H}. \quad (12)$$

Due to the fact that the increments of FBM are stationary, the variance of Eq. (12) depends only on the length Δ of the temporal interval $[t, t + \Delta]$.

Using the fact that FIM is a selfsimilar process with Hurst exponent H , as well as the fact that FIM is a martingale, it is shown in the Methods that the FIM increment $I_H(t + \Delta) - I_H(t)$ is a random variable with mean zero and with variance

$$\mathbf{Var}[I_H(t + \Delta) - I_H(t)] = \mathbf{Var}[I_H(1)] \cdot [(t + \Delta)^{2H} - t^{2H}]. \quad (13)$$

The variance of Eq. (13) depends on the starting point t , as well as on the length Δ , of the temporal interval $[t, t + \Delta]$. Hence, Eq. (13) implies that the increments of FIM are *not* stationary.

The asymptotic behavior of the variance of Eq. (13), in the temporal limit $t \rightarrow \infty$, is $\mathbf{Var}[I_H(t + \Delta) - I_H(t)] \approx v \cdot t^{2H-1}$, where $v = \mathbf{Var}[I_H(1)] \cdot 2\Delta^H$ (see the Methods for the details of this asymptotic equivalence). Consequently, for sub-diffusion ($0 < H < \frac{1}{2}$) Eq. (13) implies that: $\lim_{t \rightarrow \infty} \mathbf{Var}[I_H(t + \Delta) - I_H(t)] = 0$; namely, the variance of the FIM increment $I_H(t + \Delta) - I_H(t)$ vanishes in the temporal limit $t \rightarrow \infty$. And, for super-diffusion ($\frac{1}{2} < H < 1$) Eq. (13) implies that: $\lim_{t \rightarrow \infty} \mathbf{Var}[I_H(t + \Delta) - I_H(t)] = \infty$; namely, the variance of the FIM $I_H(t + \Delta) - I_H(t)$ increment explodes in the temporal limit $t \rightarrow \infty$.

Evidently, the difference between the variance of Eq. (12) and the variance of Eq. (13) is dramatic. Indeed, consider an observation that starts at the time point t , and whose length is Δ ; also, address t as the ‘age’ of the observation. On the one hand, the ‘age’ of the observation has no effect when observing BM and FBM. On the other hand, the ‘age’ of the observation has a profound effect when observing FIM: the statistical fluctuations of the FIM increment become smaller and smaller with ‘age’ when the FIM is sub-diffusive; and the statistical fluctuations of the FIM increment become larger and larger with ‘age’ when the FIM is super-diffusive.

3.6 Correlation comparison

In this last comparison between FBM and FIM, we examine the correlations of their velocities. To that end we set two positive and distinct time points, t_1 and t_2 , and address the covariance of their velocities at these points.

As FBM is a selfsimilar process with Hurst exponent H , and as its increments are stationary, it follows that the covariance of the FBM positions $B_H(t_1)$ and $B_H(t_2)$ is [2]:

$$\mathbf{Cov}[B_H(t_1), B_H(t_2)] = \frac{1}{2} \mathbf{Var}[B_H(1)] \cdot \left(t_1^{2H} - |t_1 - t_2|^{2H} + t_2^{2H} \right) . \quad (14)$$

Differentiating the covariance of Eq. (14) with respect to the temporal variable t_1 , and then with respect to the temporal variable t_2 , implies that the covariance of the FBM velocities $\dot{B}_H(t_1)$ and $\dot{B}_H(t_2)$ is:

$$\mathbf{Cov}[\dot{B}_H(t_1), \dot{B}_H(t_2)] = \mathbf{Var}[B_H(1)] \cdot \frac{H(2H-1)}{|t_1 - t_2|^{2(1-H)}} . \quad (15)$$

The covariance of Eq. (15) has the following implications. For sub-diffusion ($0 < H < \frac{1}{2}$) the FBM velocities are negatively correlated: $\mathbf{Cov}[\dot{B}_H(t_1), \dot{B}_H(t_2)] < 0$. For super-diffusion ($\frac{1}{2} < H < 1$) the FBM velocities are positively correlated: $\mathbf{Cov}[\dot{B}_H(t_1), \dot{B}_H(t_2)] > 0$. And, for regular diffusion ($H = \frac{1}{2}$) – in which case FBM is BM – the FBM velocities are uncorrelated: $\mathbf{Cov}[\dot{B}_H(t_1), \dot{B}_H(t_2)] = 0$.

As FIM is a selfsimilar process with Hurst exponent H , and as it is a martingale, it is shown in the Methods (see Eq. (51)) that the covariance of the FIM positions $I_H(t_1)$ and $I_H(t_2)$ is:

$$\mathbf{Cov}[I_H(t_1), I_H(t_2)] = \mathbf{Var}[I_H(1)] \cdot (\min\{t_1, t_2\})^{2H} . \quad (16)$$

Differentiating the covariance of Eq. (16) with respect to the temporal variable t_1 , and then with respect to the temporal variable t_2 , implies that the covariance of the FIM velocities $\dot{I}_H(t_1)$ and $\dot{I}_H(t_2)$ is zero:

$$\mathbf{Cov}[\dot{I}_H(t_1), \dot{I}_H(t_2)] = 0 . \quad (17)$$

Namely, the FIM velocities $\dot{I}_H(t_1)$ and $\dot{I}_H(t_2)$ are uncorrelated.

Evidently, the difference between the velocities covariance of Eq. (15) and the velocities covariance of Eq. (17) is dramatic. On the one hand, changing the Hurst exponent H in the FBM model has a profound effect, both qualitatively and quantitatively, on the correlations of the FBM velocities. On the other hand, changing the Hurst exponent H in the FIM model has no effect on the correlations of the FIM velocities – as these velocities are always uncorrelated.

4 Diffusion in a logarithmic potential

As described above, the Ito stochastic dynamics of FIM have a zero drift and a position-dependent volatility. Namely, the evolution of FIM is governed by

an Ito stochastic differential equation (SDE) of the form $\dot{X}(t) = \sigma[X(t)]\dot{B}(t)$. Many researchers in the physical sciences and in engineering are used to work with Langevin stochastic dynamics [95]-[97], which have a position-dependent drift and a constant volatility. Up to an inherent time scale, the latter evolution is governed by a Langevin SDE of the form $\dot{X}(t) = \mu[X(t)] + \dot{B}(t)$.

As noted above, a special case of the FIM model was investigated in [30]: in this special case the motion runs over the positive half-line ($0 < x < \infty$), and the Hurst exponent is in the range $\frac{1}{2} \leq H < 1$. It was shown in [30] that the special case of FIM admits a Langevin representation. In this section we shall present a Langevin representation for the (general) FIM model.

There is a one-to-one mapping between FIM and a particular random motion that is generated by specific Langevin stochastic dynamics. Indeed, map the FIM trajectory $I_H(t)$ ($t \geq 0$) to the trajectory $\xi_H(t)$ ($t \geq 0$) via the following transformation: $\xi_H(t) = \varphi[I_H(t)]$, where $\varphi(x) = 2H|x|^{1/2H} \text{sign}(x)$, and where $\text{sign}(x)$ is the sign of x .¹ Then, using Ito's formula and Eq. (4), it is shown in the Methods that the stochastic dynamics of the random motion $\xi_H(t)$ are governed by the Langevin SDE

$$\dot{\xi}_H(t) = \left(\frac{1}{2} - H\right) \frac{1}{\xi_H(t)} + \dot{B}(t) . \quad (18)$$

Shifting back from the trajectory $\xi_H(t)$ ($t \geq 0$) to the FIM trajectory $I_H(t)$ ($t \geq 0$) is via the corresponding inverse transformation: $I_H(t) = \varphi^{-1}[\xi_H(t)]$, where $\varphi^{-1}(y) = (\frac{1}{2H}|y|)^{2H} \text{sign}(y)$.

The drift of the Langevin SDE (18) is harmonic, $\mu(x) = (\frac{1}{2} - H)/x$. This drift underscores and highlights the three different diffusivity categories of FIM – which are determined by the value of its Hurst exponent H . When FIM is sub-diffusive ($0 < H < \frac{1}{2}$) then the Langevin drift is ‘repulsive’: it pushes *away* from the spatial origin. When FIM is super-diffusive ($\frac{1}{2} < H < 1$) then the Langevin drift is ‘attractive’: it pushes *towards* the spatial origin. And when FIM is a regular diffusion ($H = \frac{1}{2}$) then the Langevin drift is zero.

A Langevin SDE of the form $\dot{X}(t) = \mu[X(t)] + \dot{B}(t)$ is commonly characterized by its “potential function”: a function $U(x)$ whose negative gradient is the drift, $-U'(x) = \mu(x)$. The potential function $U(x)$ manifests a ‘potential landscape’ that underpins and governs the Langevin stochastic dynamics. The random motions that are generated by a Langevin SDE with a logarithmic potential $U(x) = r \cdot \ln(|x|)$ – where r is a real parameter – are termed “diffusion in a logarithmic potential” (DLP). The topic of DLP attracted significant scientific interest recently [120]-[129].

Arguably, the best known example of DLP is the Bessel process [130]-[134]: the Euclidean distance of a Brownian motion – which takes place in the d -dimensional Euclidean space – from the space’s origin. In this example DLP runs over the positive half-line ($0 < x < \infty$), and its parameter is $r = \frac{1}{2}(d - 1)$. So, for dimensions $d = 2, 3, 4, 5, 6, \dots$, the Bessel process yields the DLP parameter values $r = \frac{1}{2}, \frac{2}{2}, \frac{3}{2}, \frac{4}{2}, \frac{5}{2}, \dots$.

¹Namely, $\text{sign}(x) = 1$ if x is positive, and $\text{sign}(x) = -1$ if x is negative.

FIM yields – via the Langevin SDE (18) – another example of DLP. Indeed, the underpinning potential function of the Langevin SDE (18) is logarithmic with parameter $r = H - \frac{1}{2}$. As the Hurst exponent of FIM takes values in the range $0 < H < 1$, the corresponding DLP parameter takes values in the range $-\frac{1}{2} < r < \frac{1}{2}$. Negative values of the DLP parameter correspond to sub-diffusive FIM, and positive values of the DLP parameter correspond to super-diffusive FIM.

As noted above, the potential function $U(x)$ manifests the ‘potential landscape’ that underpins and governs the Langevin SDE $\dot{X}(t) = \mu[X(t)] + \dot{B}(t)$. Analogously, the volatility function $\sigma(x)$ manifests the ‘volatility landscape’ that underpins and governs the drift-less Ito SDE $\dot{X}(t) = \sigma[X(t)]\dot{B}(t)$. The one-to-one mapping between FIM and its corresponding DLP induces a one-to-one mapping between their respective underpinning landscapes: the power-law volatility landscape $\sigma(x) = |x|^{1-\frac{1}{2H}}$, and the logarithmic potential landscape $U(x) = (H - \frac{1}{2}) \ln(|x|)$. Schematic illustrations of these corresponding landscapes are depicted in Figure 8.

5 Summary

Setting off from the paradigmatic model for regular diffusion, *Brownian motion* (BM), in this paper we examined and compared two anomalous-diffusion models that generalize BM: the popular and well-known *fractional Brownian motion* (FBM) model, and the *fractional Ito motion* (FIM) model. A ‘bird’s-eye view’ of FBM vs. FIM is summarized in Table 3. More specifically, going over a list of key BM properties, Table 3: compares FBM and FIM to BM; and compares FBM to FIM.

From the perspective of mean-square-displacement measurements, both FBM and FIM exhibit the very same modeling ‘efficacy’. Indeed, in both these models the range of the Hurst exponent is $0 < H < 1$. Consequently, both these models yield: sub-diffusion in the Hurst range $0 < H < \frac{1}{2}$; super-diffusion in the Hurst range $\frac{1}{2} < H < 1$; and regular diffusion at the Hurst value $H = \frac{1}{2}$ – in which case both FBM and FIM are BM. Thus, the FBM and FIM models are indistinguishable from the mean-square-displacement perspective.

However, the stochastic propagation mechanisms of FBM and FIM are dramatically different. On the one hand, the FBM velocity (Eq. (2)) is a linear moving average of the underlying white noise – where the averaging is temporal, and it goes from the present (the time point t) all the way back to the infinitely distant past (the time point $-\infty$). We emphasize that the FBM velocity does not depend on the FBM positions. On the other hand, the FIM velocity (Eq. (4)) is a non-linear mapping of the following present (the time point t) quantities: the present FIM position, and the present value of the underlying white noise.

The profound differences between FBM and FIM – which are evident from Table 3, and moreover from the detailed comparisons of section 3 – stem from

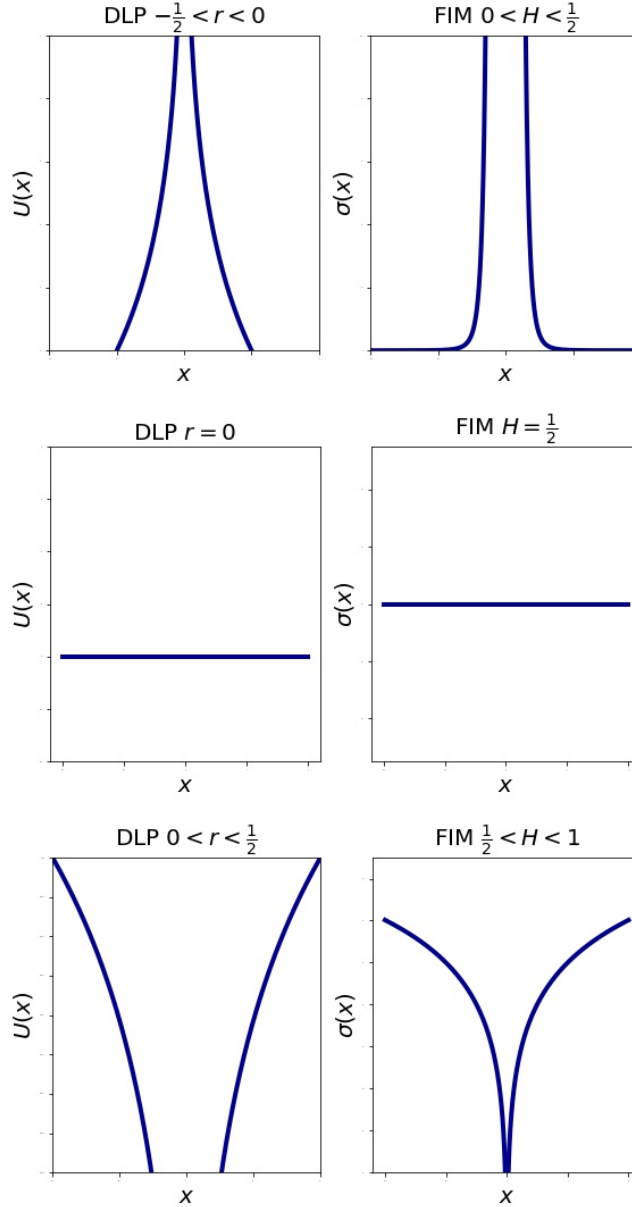


Figure 8: schematic illustrations of the shapes of the FIM volatility landscape, and of the corresponding DLP potential landscape. Depicted in the right panels, the FIM volatility landscape is: $\sigma(x) = |x|^{1-\frac{1}{2H}}$ over the spatial axis $-\infty < x < \infty$. Depicted in the left panels, the DLP potential landscape is: $U(x) = r \cdot \ln(|x|)$ over the spatial axis $-\infty < x < \infty$. The one-to-one correspondence between the two landscapes is via the relation $r = H - \frac{1}{2}$, where $0 < H < 1$ and $-\frac{1}{2} < r < \frac{1}{2}$. The two landscapes display markedly different shapes in the three different diffusivity categories: sub-diffusion $0 < H < \frac{1}{2}$ and $-\frac{1}{2} < r < 0$ (top panels); super-diffusion $\frac{1}{2} < H < 1$ and $0 < r < \frac{1}{2}$ (bottom panels); and regular diffusion $H = \frac{1}{2}$ and $r = 0$ (middle panels).

the dramatic differences between the stochastic propagation mechanisms of these anomalous-diffusion models. Due to its properties, FBM is a rather challenging model from the perspectives of numerical simulation, of stochastic integration, and of analytic tractability. Conversely, from these very perspectives, FIM is a compelling and an amicable working model.

In addition to FIM being a potent model for anomalous diffusion, we showed that there is a one-to-one mapping between FIM and diffusion in a logarithmic potential (where the coefficient of the logarithmic potential is $H - \frac{1}{2}$). With its compelling properties, its easy numerical simulation, its analytic tractability, and its linkage to diffusion in a logarithmic potential – we believe that FIM may become a prevalent working model for anomalous diffusion in various fields of science and engineering.

Table 3

	BM	FBM	FIM
Finite variance	YES		
Symmetric process	YES		
Continuous trajectory	YES		
Selfsimilar process	YES		
Hurst exponent	$H = \frac{1}{2}$	$0 < H < 1$	$0 < H < 1$
Gaussian process	YES	YES	NO
Markov process	YES	NO	YES
Martingale	YES	NO	YES
Stationary increments	YES	YES	NO
Uncorrelated increments	YES	NO	YES

Table 3: a ‘bird’s-eye view’ comparison between the FBM and FIM models with Hurst exponents $H \neq \frac{1}{2}$. The comparison is with respect to the ‘benchmark’ BM model – which the FBM and FIM models yield at the Hurst exponent $H = \frac{1}{2}$. Each row of the table specifies a different key property of BM. The top four rows of the table highlight the properties that FBM and FIM share in common with BM. The bottom six rows of the table underscore the marked differences between the three models (the last row of the table refers to non-overlapping increments).

6 Methods

6.1 The macroscopic power-law structure of the MSD function

Consider a one-dimensional random motion whose trajectory is $X(t)$ ($t \geq 0$). Given a positive number n , speed up the temporal scale by the factor n . To compensate for speeding up time, shrink the spatial scale by the positive factor $\varphi(n)$ (which is a continuous function of the positive number n). This spatio-temporal scaling shifts the trajectory $X(t)$ ($t \geq 0$) to the trajectory $X_n(t)$ ($t \geq 0$), where

$$X_n(t) = \frac{1}{\varphi(n)} X(nt) . \quad (19)$$

The MSD function of the random motion is $\phi(t) = \mathbf{E}[|X(t) - X(0)|^2]$. In turn, the MSD function of the scaled random motion is

$$\begin{aligned} \phi_n(t) &= \mathbf{E} \left[|X_n(t) - X_n(0)|^2 \right] \\ &= \mathbf{E} \left[\left| \frac{1}{\varphi(n)} X(nt) - \frac{1}{\varphi(n)} X(n0) \right|^2 \right] \\ &= \frac{1}{\varphi(n)^2} \mathbf{E} \left[|X(nt) - X(0)|^2 \right] \\ &= \frac{\phi(nt)}{\varphi(n)^2} . \end{aligned} \quad (20)$$

This MSD function can be written as follows

$$\phi_n(t) = \frac{\phi(n)}{\varphi(n)^2} \cdot \frac{\phi(nt)}{\phi(n)} . \quad (21)$$

Now, consider the MSD function $\phi_n(t)$ in the scaling limit $n \rightarrow \infty$. In general, in order to obtain a non-trivial point-wise limit $\phi_\infty(t) = \lim_{n \rightarrow \infty} \phi_n(t)$ (for any positive time t), two conditions must be met. Firstly, the spatial scaling function $\varphi(n)$ should be asymptotically equivalent (in the limit $n \rightarrow \infty$) to the function $\sqrt{\phi(n)}$. Secondly, the MSD function $\phi(t)$ should be regularly varying at infinity [135]. If these two conditions hold then the non-trivial point-wise limit is

$$\phi_\infty(t) = c \cdot t^\epsilon , \quad (22)$$

where: c is a positive constant that stems from the first condition; and ϵ is a positive regular-variation exponent that stems from the second condition.

6.2 The CV scores of FBM and FIM

We start with the random variable

$$Z = 2H^2 \cdot |I_H(1)|^{1/H} . \quad (23)$$

The cumulative distribution function of the random variable Z is

$$\begin{aligned}
\Pr(Z \leq z) &= \Pr\left(2H^2 \cdot |I_H(1)|^{1/H} \leq z\right) \\
&= \Pr\left[|I_H(1)| \leq \left(\frac{z}{2H^2}\right)^H\right] \\
&= 2\Pr\left[I_H(1) \leq \left(\frac{z}{2H^2}\right)^H\right] - 1
\end{aligned} \tag{24}$$

($z \geq 0$). In the transition from the second line of Eq. (24) to the third line we used the fact that the random variable $I_H(1)$ is symmetric (i.e., the random variable $I_H(1)$ is equal in law to the random variable $-I_H(1)$).

Denote by $g(z)$ ($z \geq 0$) the density function of the random variable Z , and denote by $f(x)$ ($-\infty < x < \infty$) the density function of the random variable $I_H(1)$. Differentiating Eq. (24), and then using the density function of Eq. (7), implies that

$$\begin{aligned}
g(z) &= 2f\left[\left(\frac{z}{2H^2}\right)^H\right] \frac{1}{(2H^2)^H} H z^{H-1} \\
&= \frac{2H}{(2H^2)^H} f\left[\left(\frac{z}{2H^2}\right)^H\right] z^{H-1} \\
&= \frac{2H}{(2H^2)^H} \left\{ \frac{H^{1-2H}}{2^H \Gamma(1-H)} \exp\left[-2H^2 \left|\left(\frac{z}{2H^2}\right)^H\right|^{\frac{1}{H}}\right] \left|\left(\frac{z}{2H^2}\right)^H\right|^{\frac{1}{H}-2}\right\} z^{H-1} \\
&= \left\{ \frac{2H}{(2H^2)^H} \frac{H^{1-2H}}{2^H \Gamma(1-H)} \frac{1}{(2H^2)^{1-2H}} \right\} \exp(-z) \{z^{1-2H} z^{H-1}\} \\
&= \frac{1}{\Gamma(1-H)} \exp(-z) z^{-H} .
\end{aligned} \tag{25}$$

In turn, Eq. (25) implies that

$$g(z) = \frac{1}{\Gamma(1-H)} \exp(-z) z^{(1-H)-1} . \tag{26}$$

The density function of Eq. (26) characterizes a Gamma distribution with Gamma exponent $1-H$. Consequently, the mean of the random variable Z^p – where p is a positive power – is

$$\mathbf{E}[Z^p] = \frac{\Gamma(1-H+p)}{\Gamma(1-H)} . \tag{27}$$

Eq. (23) implies that

$$|I_H(1)| = \left(\frac{1}{2H^2}\right)^H \cdot Z^H . \tag{28}$$

In turn, for any inequality index \mathcal{I} we have

$$\mathcal{I}(|I_H(1)|) = \mathcal{I}(Z^H) . \tag{29}$$

In particular, for the inequality index \mathcal{I} that yields the CV score we have

$$\begin{aligned}
\mathcal{I}(|I_H(1)|) &= 1 - \frac{\mathbf{E}[Z^H]^2}{\mathbf{E}[Z^{2H}]} \\
&= 1 - \frac{\left[\frac{\Gamma(1-H+H)}{\Gamma(1-H)}\right]^2}{\left[\frac{\Gamma(1-H+2H)}{\Gamma(1-H)}\right]} = 1 - \frac{\Gamma(1)^2}{\Gamma(1+H)\Gamma(1-H)} \\
&= 1 - \frac{1}{H\Gamma(H)\Gamma(1-H)} = 1 - \frac{1}{H} \frac{1}{\Gamma(H)\Gamma(1-H)} \\
&= 1 - \frac{1}{H} \frac{\sin(\pi H)}{\pi} = 1 - \frac{\sin(\pi H)}{\pi H} .
\end{aligned} \tag{30}$$

In Eq. (30) we used the following (well known) properties of the Gamma function: $\Gamma(1) = 1$; $\Gamma(1+H) = H\Gamma(H)$; and $\Gamma(H)\Gamma(1-H) = \pi/\sin(\pi H)$. Eq. (30) proves Eq. (9).

As noted above, at the Hurst exponent $H = \frac{1}{2}$ the random variable $I_{1/2}(1)$ is “standard Normal”, i.e. it is a Normal random variable with mean zero and with variance one. Also, as noted above, the random variable $B_H(1)$ is Normal with mean zero and with variance $b = \mathbf{Var}[B_H(1)]$. Hence, the random variables $I_{1/2}(1)$ and $B_H(1)$ differ only by a scale factor:

$$B_H(1) = \sqrt{b} \cdot I_{1/2}(1) , \tag{31}$$

where the equality is in law. In turn, any inequality index \mathcal{I} will assign the random variables $|I_{1/2}(1)|$ and $|B_H(1)|$ the same statistical-heterogeneity score. In particular, for the CV score Eq. (30) implies that

$$\begin{aligned}
\mathcal{I}(|B_H(1)|) &= \mathcal{I}(|I_{1/2}(1)|) \\
&= 1 - \frac{\sin(\pi \frac{1}{2})}{\pi \frac{1}{2}} = 1 - \frac{2}{\pi} .
\end{aligned} \tag{32}$$

Eq. (32) proves Eq. (8).

6.3 The Kulback-Leibler divergence of FBM and FIM

Consider a one-dimensional random motion whose trajectory is $X(t)$ ($t \geq 0$), and denote by $f_t(x)$ the density of the random variable $X(t)$. As noted above, the Kulback-Leibler (KL) divergence of the random variable $X(t)$ from the random variable $X(1)$ is:

$$\mathcal{D}[X(t) || X(1)] = \int_{-\infty}^{\infty} \ln \left[\frac{f_t(x)}{f_1(x)} \right] f_t(x) dx . \tag{33}$$

6.3.1 FBM case

For FBM, Eq. (6) implies that

$$\begin{aligned} \frac{f_t(x)}{f_1(x)} &= \frac{\frac{1}{\sqrt{2\pi b}} \frac{1}{t^H} \exp\left(-\frac{x^2}{2bt^{2H}}\right)}{\frac{1}{\sqrt{2\pi b}} \exp\left(-\frac{x^2}{2b}\right)} \\ &= \frac{1}{t^H} \exp\left[\frac{x^2}{2b} \left(1 - \frac{1}{t^{2H}}\right)\right], \end{aligned} \quad (34)$$

and hence

$$\ln \left[\frac{f_t(x)}{f_1(x)} \right] = -H \ln(t) + \frac{1}{2b} \left(1 - \frac{1}{t^{2H}}\right) \cdot x^2. \quad (35)$$

Setting the random motion $X(t)$ ($t \geq 0$) to be FBM, and substituting Eq. (35) into Eq. (33) yields

$$\begin{aligned} \mathcal{D}[B_H(t) || B_H(1)] &= \int_{-\infty}^{\infty} \left[-H \ln(t) + \frac{1}{2b} \left(1 - \frac{1}{t^{2H}}\right) \cdot x^2\right] f_t(x) dx \\ &= -H \ln(t) \int_{-\infty}^{\infty} f_t(x) dx + \frac{1}{2b} \left(1 - \frac{1}{t^{2H}}\right) \int_{-\infty}^{\infty} x^2 f_t(x) dx \\ &= -H \ln(t) + \frac{1}{2b} \left(1 - \frac{1}{t^{2H}}\right) \mathbf{E} \left[B_H(t)^2 \right]. \end{aligned} \quad (36)$$

As noted above, the properties of FBM imply that the random variable $B_H(t)$ is Normal with mean zero with variance $\mathbf{Var}[B_H(t)] = b \cdot t^{2H}$ – and hence

$$\mathbf{E} \left[B_H(t)^2 \right] = b \cdot t^{2H}. \quad (37)$$

Combining Eq. (36) and Eq. (37) together, we obtain that

$$\begin{aligned} \mathcal{D}[B_H(t) || B_H(1)] &= -H \ln(t) + \frac{1}{2b} \left(1 - \frac{1}{t^{2H}}\right) bt^{2H} \\ &= \frac{1}{2} \left(t^{2H} - 1\right) - H \ln(t). \end{aligned} \quad (38)$$

Eq. (38) proves Eq. (10).

6.3.2 FIM case

For FIM, Eq. (7) implies that

$$\begin{aligned} \frac{f_t(x)}{f_1(x)} &= \frac{\frac{1}{2H\Gamma(1-H)} \cdot \left(\frac{2H^2}{t}\right)^{1-H} \exp\left(-\frac{2H^2}{t} |x|^{\frac{1}{H}}\right) |x|^{\frac{1}{H}-2}}{\frac{1}{2H\Gamma(1-H)} (2H^2)^{1-H} \exp\left(-2H^2 |x|^{\frac{1}{H}}\right) |x|^{\frac{1}{H}-2}} \\ &= \frac{1}{t^{1-H}} \exp\left[2H^2 |x|^{\frac{1}{H}} \left(1 - \frac{1}{t}\right)\right], \end{aligned} \quad (39)$$

and hence

$$\ln \left[\frac{f_t(x)}{f_1(x)} \right] = -(1-H) \ln(t) + 2H^2 \left(1 - \frac{1}{t}\right) \cdot |x|^{\frac{1}{H}} . \quad (40)$$

Setting the random motion $X(t)$ ($t \geq 0$) to be FIM, and substituting Eq. (40) into Eq. (33) yields

$$\begin{aligned} & \mathcal{D} [I_H(t) | I_H(1)] \\ &= \int_{-\infty}^{\infty} \left[-(1-H) \ln(t) + 2H^2 \left(1 - \frac{1}{t}\right) \cdot |x|^{\frac{1}{H}} \right] f_t(x) dx \\ &= -(1-H) \ln(t) \int_{-\infty}^{\infty} f_t(x) dx + 2H^2 \left(1 - \frac{1}{t}\right) \int_{-\infty}^{\infty} |x|^{\frac{1}{H}} f_t(x) dx \\ &= -(1-H) \ln(t) + 2H^2 \left(1 - \frac{1}{t}\right) \mathbf{E} \left[|I_H(t)|^{\frac{1}{H}} \right] . \end{aligned} \quad (41)$$

The selfsimilarity of FIM implies that $I_H(t) = t^H \cdot I_H(1)$ (the equality being in law), and hence

$$\begin{aligned} \mathbf{E} \left[|I_H(t)|^{\frac{1}{H}} \right] &= \mathbf{E} \left[|t^H \cdot I_H(1)|^{\frac{1}{H}} \right] \\ &= \mathbf{E} \left[t \cdot |I_H(1)|^{\frac{1}{H}} \right] = t \cdot \mathbf{E} \left[|I_H(1)|^{\frac{1}{H}} \right] . \end{aligned} \quad (42)$$

Using Eq. (7), and setting $\lambda = 2H^2$, note that the density of the random variable $|I_H(1)|$ is

$$\frac{\lambda^{1-H}}{H\Gamma(1-H)} \exp\left(-\lambda x^{\frac{1}{H}}\right) x^{\frac{1}{H}-2} \quad (43)$$

($0 < x < \infty$), and hence (using the change-of-variables $y = \lambda x^{\frac{1}{H}}$):

$$\begin{aligned} & \mathbf{E} \left[|I_H(1)|^{\frac{1}{H}} \right] \\ &= \int_0^{\infty} x^{\frac{1}{H}} \cdot \frac{\lambda^{1-H}}{H\Gamma(1-H)} \exp\left(-\lambda x^{\frac{1}{H}}\right) x^{\frac{1}{H}-2} dx \\ &= \frac{\lambda^{1-H}}{H\Gamma(1-H)} \int_0^{\infty} \exp\left(-\lambda x^{\frac{1}{H}}\right) x^{\frac{2}{H}-2} dx \\ &= \frac{1}{\lambda\Gamma(1-H)} \int_0^{\infty} \exp(-y) y^{(2-H)-1} dy \\ &= \frac{1}{\lambda\Gamma(1-H)} \Gamma(2-H) \\ &= \frac{1-H}{\lambda} = \frac{1-H}{2H^2} . \end{aligned} \quad (44)$$

Combining Eq. (41) and Eq. (42) together with Eq. (44), we obtain that

$$\begin{aligned}
& \mathcal{D}[I_H(t) || I_H(1)] \\
&= -(1-H) \ln(t) + 2H^2 \left(1 - \frac{1}{t}\right) \mathbf{E} \left[|I_H(t)|^{\frac{1}{H}} \right] \\
& \quad - (1-H) \ln(t) + 2H^2 \left(1 - \frac{1}{t}\right) \cdot t^{\frac{1-H}{2H^2}} \\
&= (1-H) [t - 1 - \ln(t)] .
\end{aligned} \tag{45}$$

Eq. (45) proves Eq. (11).

6.4 The mean and the variance of the FIM increment

Consider the FIM increment $I_H(t + \Delta) - I_H(t)$. As FIM is a symmetric process, its positions have zero means, and hence so do its increments; thus, in particular, the increment $I_H(t + \Delta) - I_H(t)$ has a zero mean. The variance of the increment $I_H(t + \Delta) - I_H(t)$ satisfies

$$\begin{aligned}
& \mathbf{Var}[I_H(t + \Delta) - I_H(t)] \\
&= \mathbf{Var}[I_H(t + \Delta)] - 2\mathbf{Cov}[I_H(t + \Delta), I_H(t)] + \mathbf{Var}[I_H(t)] .
\end{aligned} \tag{46}$$

As FIM is a selfsimilar process with Hurst exponent H , the random variable $I_H(t)$ is equal in law to the random variable $t^H \cdot I_H(1)$, and the random variable $I_H(t + \Delta)$ is equal in law to the random variable $(t + \Delta)^H \cdot I_H(1)$. Hence, setting $v_1 = \mathbf{Var}[I_H(1)]$, we have

$$\mathbf{Var}[I_H(t)] = v_1 \cdot t^{2H} , \tag{47}$$

and

$$\mathbf{Var}[I_H(t + \Delta)] = v_1 \cdot (t + \Delta)^{2H} . \tag{48}$$

The fact that the positions of FIM have zero means implies that

$$\mathbf{Cov}[I_H(t + \Delta), I_H(t)] = \mathbf{E}[I_H(t + \Delta) \cdot I_H(t)] . \tag{49}$$

Denote by \mathcal{F}_t the sigma-field generated by the trajectory of FIM over the temporal interval $[0, t]$. The martingale property of FIM implies that – given the information \mathcal{F}_t – the conditional mean of the random variable $I_H(t + \Delta)$ is: $\mathbf{E}[I_H(t + \Delta) | \mathcal{F}_t] = I_H(t)$. Hence, applying conditioning to the right-hand side of Eq. (49), and using the fact that the random variable $I_H(t)$ has a zero mean, we have

$$\begin{aligned}
& \mathbf{E}[I_H(t + \Delta) \cdot I_H(t)] = \mathbf{E}[\mathbf{E}[I_H(t + \Delta) \cdot I_H(t) | \mathcal{F}_t]] \\
&= \mathbf{E}[I_H(t) \cdot \mathbf{E}[I_H(t + \Delta) | \mathcal{F}_t]] = \mathbf{E}[I_H(t) \cdot I_H(t)] \\
&= \mathbf{E}[I_H(t)^2] = \mathbf{Var}[I_H(t)] .
\end{aligned} \tag{50}$$

Combining together Eq. (47), Eq. (49), and Eq. (50) yields

$$\mathbf{Cov} [I_H (t + \Delta), I_H (t)] = \mathbf{Var} [I_H (t)] = v_1 \cdot t^{2H} . \quad (51)$$

In turn, substituting Eqs. (47)-(48) and Eq. (51) into Eq. (46) yields

$$\begin{aligned} \mathbf{Var} [I_H (t + \Delta) - I_H (t)] \\ &= v_1 \cdot (t + \Delta)^{2H} - 2v_1 \cdot t^{2H} + v_1 \cdot t^{2H} \\ &= v_1 \cdot \left[(t + \Delta)^{2H} - t^{2H} \right] . \end{aligned} \quad (52)$$

Eq. (52) proves Eq. (13).

In the limit $t \rightarrow \infty$ note that

$$\lim_{t \rightarrow \infty} \frac{(t + \Delta)^{2H} - t^{2H}}{t^{2H-1}} = \Delta \cdot \lim_{t \rightarrow \infty} \frac{\left(1 + \frac{\Delta}{t}\right)^{2H} - 1}{\frac{\Delta}{t}} = \Delta \cdot 2H . \quad (53)$$

Hence, in the limit $t \rightarrow \infty$, Eq. (52) and Eq. (53) yield the following asymptotic equivalence:

$$\mathbf{Var} [I_H (t + \Delta) - I_H (t)] \approx (v_1 \Delta 2H) \cdot t^{2H-1} . \quad (54)$$

6.5 The linkage between FIM and Langevin stochastic dynamics

The stochastic dynamics of FIM are governed by the Ito SDE $\dot{I}_H (t) = \sigma [I_H (t)] \dot{B} (t)$, with the power-law “volatility” $\sigma (x) = |x|^{1-\frac{1}{2H}}$. Consider a monotone increasing function $\varphi (x)$ that maps the real line to the real line, and introduce the following map of FIM: the random motion $\xi_H (t) = \varphi [I_H (t)]$ ($t \geq 0$). Its formula [15] and the stochastic dynamics of FIM imply that

$$\dot{\xi}_H (t) = \frac{1}{2} \varphi'' [I_H (t)] \sigma [I_H (t)]^2 + \{ \varphi' [I_H (t)] \sigma [I_H (t)] \} \dot{B} (t) . \quad (55)$$

Our goal is that the stochastic dynamics of random motion $\xi_H (t)$ ($t \geq 0$) be governed by a Langevin SDE of the form $\dot{\xi}_H (t) = \mu \left[\xi_H (t) \right] + \dot{B} (t)$. To that end, the function $\varphi (x)$ must satisfy the condition $\varphi' (x) \sigma (x) = 1$. As $\sigma (x) = |x|^{1-\frac{1}{2H}}$, the only function $\varphi (x)$ that satisfies this condition is

$$\varphi (x) = 2H |x|^{\frac{1}{2H}} \cdot \text{sign} (x) , \quad (56)$$

where $\text{sign} (x)$ is the sign of x . Indeed, the first derivative of the function appearing in Eq. (56) is

$$\varphi' (x) = |x|^{\frac{1}{2H}-1} = \frac{1}{\sigma (x)} . \quad (57)$$

Also, the second derivative of the function appearing in Eq. (56) is

$$\varphi''(x) = \left(\frac{1}{2H} - 1 \right) |x|^{\frac{1}{2H}-2} \cdot \text{sign}(x) . \quad (58)$$

Eqs. (56)-(58) imply that

$$\begin{aligned} & \frac{1}{2} \varphi''(x) \sigma(x)^2 \\ &= \frac{1}{2} \left(\frac{1}{2H} - 1 \right) |x|^{\frac{1}{2H}-2} \cdot \text{sign}(x) \cdot |x|^{2-\frac{1}{H}} \\ &= \frac{1}{2} \left(\frac{1}{2H} - 1 \right) |x|^{-\frac{1}{2H}} \cdot \text{sign}(x) \\ &= \frac{1}{2} (1 - 2H) \frac{1}{2H|x|^{\frac{1}{2H}} \cdot \text{sign}(x)} \\ &= \left(\frac{1}{2} - H \right) \frac{1}{\varphi(x)} . \end{aligned} \quad (59)$$

In turn, substituting Eq. (57) and Eq. (59) into Eq. (55) implies that

$$\begin{aligned} \dot{\xi}_H(t) &= \left(\frac{1}{2} - H \right) \frac{1}{\varphi[\Gamma_H(t)]} + \dot{B}(t) \\ &= \left(\frac{1}{2} - H \right) \frac{1}{\xi_H(t)} + \dot{B}(t) . \end{aligned} \quad (60)$$

Eq. (60) proves Eq. (18).

References

- [1] Eliazar, Iddo Isaac. "Selfsimilar diffusions." *Journal of Physics A: Mathematical and Theoretical* (2021).
- [2] Embrechts, Paul, and Makoto Maejima. *Selfsimilar processes*. Princeton University Press, 2009.
- [3] Friedman, Avner. *Stochastic differential equations and applications*. Dover publications, 2006.
- [4] Oksendal, Bernt. *Stochastic differential equations: an introduction with applications*. Springer Science & Business Media, 2013.
- [5] Arnold, Ludwig. *Stochastic differential equations: Theory and applications*. Dover publications, 2014.
- [6] Pekalski, Andrzej, and Katarzyna Sznajd-Weron (Eds.). *Anomalous Diffusion: From Basics to Applications*. Springer, 1999.

- [7] Klafter, Joseph, and Igor M. Sokolov. First steps in random walks: from tools to applications. Oxford University Press, 2011.
- [8] Mendez, Vicenc, Daniel Campos, and Frederic Bartumeus. Stochastic foundations in movement ecology: Anomalous Diffusion, Front Propagation and Random Searches. Springer-Verlag, 2013.
- [9] Evangelista, Luiz Roberto, and Ervin Kaminski Lenzi. Fractional diffusion equations and anomalous diffusion. Cambridge University Press, 2018.
- [10] Lindenberg, Katja, Ralf Metzler, and Gleb Oshanin, eds. Chemical kinetics: beyond the textbook. World scientific, 2019.
- [11] Deng, Weihua, Ru Hou, Wanli Wang, and Pengbo Xu. Modeling anomalous diffusion: from statistics to mathematics. World Scientific, 2020.
- [12] Shlesinger, Michael F. An Unbounded Experience in Random Walks with Applications. World Scientific, 2021.
- [13] Gardiner, Crispin W. Handbook of stochastic methods. Springer, 1985.
- [14] Van Kampen, Nicolaas Godfried. Stochastic processes in physics and chemistry. North Holland, 2007.
- [15] Karatzas, Ioannis, and Steven E. Shreve. Brownian motion and stochastic calculus. Springer, 1991.
- [16] Chechkin, A. V., and V. Yu Gonchar. "Fractional Brownian motion approximation based on fractional integration of a white noise." *Chaos, Solitons & Fractals* 12, no. 2 (2001): 391-398.
- [17] Mercik, Sz. and K. Weron. "Fractional Brownian Motion as a Model of the Self-Similar Ion Channel Kinetics." *Acta Physica Polonica. Series B* 32, no. 5 (2001): 1621-1630.
- [18] Magdziarz, Marcin, Aleksander Weron, Krzysztof Burnecki, and Joseph Klafter. "Fractional Brownian motion versus the continuous-time random walk: A simple test for subdiffusive dynamics." *Physical review letters* 103, no. 18 (2009): 180602.
- [19] Jeon, Jae-Hyung, and Ralf Metzler. "Fractional Brownian motion and motion governed by the fractional Langevin equation in confined geometries." *Physical Review E* 81, no. 2 (2010): 021103.
- [20] Jeon, Jae-Hyung, A. V. Chechkin, and Ralf Metzler. "First passage behaviour of fractional Brownian motion in two-dimensional wedge domains." *EPL (Europhysics Letters)* 94, no. 2 (2011): 20008.
- [21] Burnecki, Krzysztof, Eldad Kepten, Joanna Janczura, Irena Bronshtein, Yuval Garini, and Aleksander Weron. "Universal algorithm for identification of fractional Brownian motion. A case of telomere subdiffusion." *Biophysical journal* 103, no. 9 (2012): 1839-1847.

- [22] Jeon, Jae-Hyung, Aleksei V. Chechkin, and Ralf Metzler. "First passage behavior of multi-dimensional fractional Brownian motion and application to reaction phenomena." In *First-Passage Phenomena and Their Applications*, pp. 175-202. 2014.
- [23] Sikora, Grzegorz, Krzysztof Burnecki, and Agnieszka Wyłomańska. "Mean-squared-displacement statistical test for fractional Brownian motion." *Physical Review E* 95, no. 3 (2017): 032110.
- [24] Guggenberger, Tobias, Gianni Pagnini, Thomas Vojta, and Ralf Metzler. "Fractional Brownian motion in a finite interval: correlations effect depletion or accretion zones of particles near boundaries." *New Journal of Physics* 21, no. 2 (2019): 022002.
- [25] Wang, Wei, Andrey G. Cherstvy, Aleksei V. Chechkin, Samudrajit Thapa, Flavio Seno, Xianbin Liu, and Ralf Metzler. "Fractional Brownian motion with random diffusivity: emerging residual nonergodicity below the correlation time." *Journal of Physics A: Mathematical and Theoretical* 53, no. 47 (2020): 474001.
- [26] Guggenberger, Tobias, Aleksei Chechkin, and Ralf Metzler. "Fractional Brownian motion in superharmonic potentials and non-Boltzmann stationary distributions." *Journal of Physics A: Mathematical and Theoretical* 54, no. 29 (2021): 29LT01.
- [27] Wang, Wei, Andrey Cherstvy, Holger Kantz, Ralf Metzler, and Igor Sokolov. "Time-averaging and emerging nonergodicity upon resetting of fractional Brownian motion and heterogeneous diffusion processes." *bioRxiv* (2021).
- [28] Cherstvy, Andrey, Wei Wang, Ralf Metzler, and Igor Sokolov. "Inertia triggers nonergodicity of fractional Brownian motion." *bioRxiv* (2021).
- [29] Cherstvy, Andrey G., Aleksei V. Chechkin, and Ralf Metzler. "Anomalous diffusion and ergodicity breaking in heterogeneous diffusion processes." *New Journal of Physics* 15, no. 8 (2013): 083039.
- [30] Leibovich, N., and E. Barkai. "Infinite ergodic theory for heterogeneous diffusion processes." *Physical Review E* 99, no. 4 (2019): 042138.
- [31] Lenzi, M. K., E. K. Lenzi, L. M. S. Guilherme, L. R. Evangelista, and H. V. Ribeiro. "Transient anomalous diffusion in heterogeneous media with stochastic resetting." *Physica A: Statistical Mechanics and its Applications* (2021): 126560.
- [32] Van der Pas, Peter W. "The discovery of the Brownian motion." *Scientiarum Historia: Tijdschrift voor de Geschiedenis van de Wetenschappen en de Geneeskunde* 13, no. 1 (1971): 27-35.

- [33] Brown, Robert. "XXVII. A brief account of microscopical observations made in the months of June, July and August 1827, on the particles contained in the pollen of plants; and on the general existence of active molecules in organic and inorganic bodies." *The philosophical magazine* 4, no. 21 (1828): 161-173.
- [34] Perrin, Jean. "Mouvement Brownien et realite moleculaire." *Annales de Chimie et de Physique* 18 (1909): 5-104.
- [35] Scher, H., and M. Lax. "Continuous time random walk model of hopping transport: application to impurity conduction." *Journal of Non-Crystalline Solids* 8 (1972): 497-504.
- [36] Scher, Harvey, and Melvin Lax. "Stochastic transport in a disordered solid. I. Theory." *Physical Review B* 7, no. 10 (1973): 4491.
- [37] Scher, Harvey, and Melvin Lax. "Stochastic transport in a disordered solid. II. Impurity conduction." *Physical Review B* 7, no. 10 (1973): 4502.
- [38] Shlesinger, Michael F. "Asymptotic solutions of continuous-time random walks." *Journal of Statistical Physics* 10, no. 5 (1974): 421-434.
- [39] Scher, Harvey, and Elliott W. Montroll. "Anomalous transit-time dispersion in amorphous solids." *Physical Review B* 12, no. 6 (1975): 2455.
- [40] Gefen, Yuval, Amnon Aharony, and Shlomo Alexander. "Anomalous diffusion on percolating clusters." *Physical Review Letters* 50, no. 1 (1983): 77.
- [41] Klafter, Joseph, Alexander Blumen, and Michael F. Shlesinger. "Stochastic pathway to anomalous diffusion." *Physical Review A* 35, no. 7 (1987): 3081.
- [42] Bouchaud, Jean-Philippe, and Antoine Georges. "Anomalous diffusion in disordered media: statistical mechanisms, models and physical applications." *Physics reports* 195, no. 4-5 (1990): 127-293.
- [43] Zhanette, Damian H., and Pablo A. Alemany. "Thermodynamics of anomalous diffusion." *Physical review letters* 75, no. 3 (1995): 366.
- [44] Metzler, Ralf, and Joseph Klafter. "The random walk's guide to anomalous diffusion: a fractional dynamics approach." *Physics reports* 339, no. 1 (2000): 1-77.
- [45] Sokolov, Igor M., and Joseph Klafter. "From diffusion to anomalous diffusion: a century after Einstein's Brownian motion." *Chaos: An Interdisciplinary Journal of Nonlinear Science* 15, no. 2 (2005): 026103.
- [46] Klafter, Joseph, and Igor M. Sokolov. "Anomalous diffusion spreads its wings." *Physics world* 18, no. 8 (2005): 29.

- [47] Sokolov, Igor M. "Models of anomalous diffusion in crowded environments." *Soft Matter* 8, no. 35 (2012): 9043-9052.
- [48] Metzler, Ralf, Jae-Hyung Jeon, Andrey G. Cherstvy, and Eli Barkai. "Anomalous diffusion models and their properties: non-stationarity, non-ergodicity, and ageing at the centenary of single particle tracking." *Physical Chemistry Chemical Physics* 16, no. 44 (2014): 24128-24164.
- [49] dos Santos, Maíke AF. "Analytic approaches of the anomalous diffusion: A review." *Chaos, Solitons & Fractals* 124 (2019): 86-96.
- [50] Metzler, Ralf. "Brownian motion and beyond: first-passage, power spectrum, non-Gaussianity, and anomalous diffusion." *Journal of Statistical Mechanics: Theory and Experiment* 2019, no. 11 (2019): 114003.
- [51] Sancho, Jose Maria, A. M. Lacasta, Katja Lindenberg, Igor M. Sokolov, and A. H. Romero. "Diffusion on a solid surface: Anomalous is normal." *Physical review letters* 92, no. 25 (2004): 250601.
- [52] Eliazar, Iddo, and Joseph Klafter. "Anomalous is ubiquitous." *Annals of Physics* 326, no. 9 (2011): 2517-2531.
- [53] Vitali, S., Sposini, V., Sliusarenko, O., Paradisi, P., Castellani, G., & Pagnini, G. (2018). Langevin equation in complex media and anomalous diffusion. *Journal of The Royal Society Interface*, 15(145), 20180282.
- [54] Oliveira, Fernando A., Rogelma Ferreira, Luciano C. Lapas, and Mendeli H. Vainstein. "Anomalous diffusion: A basic mechanism for the evolution of inhomogeneous systems." *Frontiers in Physics* 7 (2019): 18.
- [55] Sato, Yuzuru, and Rainer Klages. "Anomalous diffusion in random dynamical systems." *Physical review letters* 122, no. 17 (2019): 174101.
- [56] Bo, Stefano, Falko Schmidt, Ralf Eichhorn, and Giovanni Volpe. "Measurement of anomalous diffusion using recurrent neural networks." *Physical Review E* 100, no. 1 (2019): 010102.
- [57] Wang, Wei, Andrey G. Cherstvy, Xianbin Liu, and Ralf Metzler. "Anomalous diffusion and nonergodicity for heterogeneous diffusion processes with fractional Gaussian noise." *Physical Review E* 102, no. 1 (2020): 012146.
- [58] Feng, Libo, Ian Turner, Patrick Perre, and Kevin Burrage. "An investigation of nonlinear time-fractional anomalous diffusion models for simulating transport processes in heterogeneous binary media." *Communications in Nonlinear Science and Numerical Simulation* 92 (2021): 105454.
- [59] Cherstvy, Andrey G., Hadiseh Safdari, and Ralf Metzler. "Anomalous diffusion, nonergodicity, and ageing for exponentially and logarithmically time-dependent diffusivity: striking differences for massive versus massless particles." *Journal of Physics D: Applied Physics* 54, no. 19 (2021): 195401.

- [60] Kononovicius, A. "Noisy voter model for the anomalous diffusion of parliamentary presence." *Journal of Statistical Mechanics: Theory and Experiment* 2020, no. 6 (2020): 063405.
- [61] Kazakevičius, Rytis, and Aleksejus Kononovicius. "Anomalous diffusion in nonlinear transformations of the noisy voter model." *Physical Review E* 103, no. 3 (2021): 032154.
- [62] Masoliver, Jaume, and Miquel Montero. "Anomalous diffusion under stochastic resettings: A general approach." *Physical Review E* 100, no. 4 (2019): 042103.
- [63] Antonio Faustino dos Santos, Maïke. "Comb model with non-static stochastic resetting and anomalous diffusion." *Fractal and Fractional* 4, no. 2 (2020): 28.
- [64] Dzhanoev, A. R., and I. M. Sokolov. "The effect of the junction model on the anomalous diffusion in the 3D comb structure." *Chaos, Solitons & Fractals* 106 (2018): 330-336.
- [65] Lenzi, E. K., T. Sandev, H. V. Ribeiro, P. Jovanovski, A. Iomin, and L. Kocarev. "Anomalous diffusion and random search in xyz-comb: exact results." *Journal of Statistical Mechanics: Theory and Experiment* 2020, no. 5 (2020): 053203.
- [66] Antonio Faustino dos Santos, Maïke. "Comb model with non-static stochastic resetting and anomalous diffusion." *Fractal and Fractional* 4, no. 2 (2020): 28.
- [67] Iomin, A. "Anomalous diffusion in umbrella comb." *Chaos, Solitons & Fractals* 142 (2021): 110488.
- [68] Wang, Wei, Flavio Seno, Igor M. Sokolov, Aleksei V. Chechkin, and Ralf Metzler. "Unexpected crossovers in correlated random-diffusivity processes." *New Journal of Physics* 22, no. 8 (2020): 083041.
- [69] @ Wang, Wei, Andrey G. Cherstvy, Aleksei V. Chechkin, Samudrajit Thapa, Flavio Seno, Xianbin Liu, and Ralf Metzler. "Fractional Brownian motion with random diffusivity: emerging residual nonergodicity below the correlation time." *Journal of Physics A: Mathematical and Theoretical* 53, no. 47 (2020): 474001.
- [70] Grebenkov, Denis S., Vittoria Sposini, Ralf Metzler, Gleb Oshanin, and Flavio Seno. "Exact first-passage time distributions for three random diffusivity models." *Journal of Physics A: Mathematical and Theoretical* 54, no. 4 (2021): 04LT01.
- [71] dos Santos, Maïke AF, and Luiz Menon Junior. "Random diffusivity models for scaled Brownian motion." *Chaos, Solitons & Fractals* 144 (2021): 110634.

- [72] Bachelier, Louis. "Theorie de la speculation." In *Annales scientifiques de l'ecole normale superieure*, vol. 17, pp. 21-86. 1900.
- [73] Bachelier, Louis. *Louis Bachelier's theory of speculation: the origins of modern finance*. Princeton University Press, 2011.
- [74] Einstein, Albert. "Uber die von der molekularkinetischen theorie der warmegeforderte bewegung von in ruhenden flussigkeitensuspendierten teilchen." *Annalen der physik* 4 (1905).
- [75] Von Smoluchowski, Marian. "Zurkinetiscentheorie der brownschen molekularbewegung und der suspensionen." *Annalen der physik* 326, no. 14 (1906): 756-780.
- [76] Wiener, Norbert. "Differential-Space." *Journal of Mathematics and Physics* 2, no. 1-4 (1923): 131-174.
- [77] Kolmogorov, Andrei Nikolaevitch. "The Wiener spiral and some other interesting curves in Hilbert space." In *Dokl. Akad. Nauk SSSR*, vol. 26, no. 2 (1940): 115-118.
- [78] Yaglom, A. M. "Correlation theory of processes with stationary increments of order n" *Amer. Math. Soc. Transl. Series, American Math. Soc. Providence RI* 8 (1958): 87-102.
- [79] Mandelbrot, Benoit B., and John W. Van Ness. "Fractional Brownian motions, fractional noises and applications." *SIAM review* 10, no. 4 (1968): 422-437.
- [80] Yuliya Mishura. *Stochastic calculus for fractional Brownian motion and related processes*. Springer Science & Business Media, 2008.
- [81] Biagini, Francesca, Yaozhong Hu, Bernt Oksendal, and Tusheng Zhang. *Stochastic calculus for fractional Brownian motion and applications*. Springer Science & Business Media, 2008.
- [82] Nourdin, Ivan. *Selected aspects of fractional Brownian motion*. Springer, 2012.
- [83] Banna, Oksana, Yuliya Mishura, Kostiantyn Ralchenko, and Sergiy Shklyar. *Fractional Brownian Motion: Approximations and Projections*. John Wiley & Sons, 2019.
- [84] Eliazar, Iddo I., and Michael F. Shlesinger. "Fractional motions." *Physics Reports* 527, no. 2 (2013): 101-129.
- [85] Yin, Z-M. "New methods for simulation of fractional Brownian motion." *Journal of computational physics* 127, no. 1 (1996): 66-72.

- [86] Jean-Francois, Coeurjolly. "Simulation and identification of the fractional Brownian motion: a bibliographical and comparative study." *Journal of statistical software* 5 (2000): 1-53.
- [87] Stein, Michael L. "Fast and exact simulation of fractional Brownian surfaces." *Journal of Computational and Graphical Statistics* 11, no. 3 (2002): 587-599.
- [88] Dieker, Antonius Bernardus, and Michael Mandjes. "On spectral simulation of fractional Brownian motion." *Probability in the Engineering and Informational Sciences* 17, no. 3 (2003): 417-434.
- [89] Dieker, Ton. "Simulation of fractional Brownian motion." PhD diss., Masters Thesis, Department of Mathematical Sciences, University of Twente, The Netherlands, 2004.
- [90] Pipiras, Vladas. "Wavelet-based simulation of fractional Brownian motion revisited." *Applied and Computational Harmonic Analysis* 19, no. 1 (2005): 49-60.
- [91] Pashko, Anatolii. "Accuracy of simulation of fractional Brownian motion." *Information Technologies, Management and Society* (2018).
- [92] Pashko, Anatolii, Olga Sinyavska, and Tetiana Oleshko. "Simulation of Fractional Brownian Motion and Estimation of Hurst Parameter." In *2020 IEEE 15th International Conference on Advanced Trends in Radioelectronics, Telecommunications and Computer Engineering (TCSET)*, pp. 632-637. IEEE, 2020.
- [93] Chen, Yi, Jing Dong, and Hao Ni. " ϵ -Strong Simulation of Fractional Brownian Motion and Related Stochastic Differential Equations." *Mathematics of Operations Research* (2021).
- [94] Shahnazi-Pour, A., B. Parsa Moghaddam, and Afshin Babaei. "Numerical simulation of the Hurst index of solutions of fractional stochastic dynamical systems driven by fractional Brownian motion." *Journal of Computational and Applied Mathematics* 386 (2021): 113210.
- [95] Langevin, Paul. "Sur la theorie du mouvement Brownien." *Compt. Rendus* 146 (1908): 530-533.
- [96] Coffey, William, and Yuri P. Kalmykov. *The Langevin equation: with applications to stochastic problems in physics, chemistry and electrical engineering*. World Scientific, 2012.
- [97] Pavliotis, Grigorios A. *Stochastic processes and applications: diffusion processes, the Fokker-Planck and Langevin equations*. Vol. 60. Springer, 2014.

- [98] Ito, Kiyosi. On stochastic differential equations. American Mathematical Soc., 1951.
- [99] Ito, Kiyosi, and P. Henry Jr. Diffusion processes and their sample paths. Springer Science & Business Media, 2012.
- [100] Hull, John C. Options, futures, and other derivatives. Pearson, 2017.
- [101] Chechkin, Aleksei V., Flavio Seno, Ralf Metzler, and Igor M. Sokolov. "Brownian yet non-Gaussian diffusion: from superstatistics to subordination of diffusing diffusivities." *Physical Review X* 7, no. 2 (2017): 021002.
- [102] Tyagi, Neha, and Binny J. Cherayil. "Non-Gaussian Brownian diffusion in dynamically disordered thermal environments." *The Journal of Physical Chemistry B* 121, no. 29 (2017): 7204-7209.
- [103] Metzler, Ralf. "Gaussianity fair: the riddle of anomalous yet non-Gaussian diffusion." *Biophysical journal* 112, no. 3 (2017): 413.
- [104] Slezak, Jakub, Ralf Metzler, and Marcin Magdziarz. "Superstatistical generalised Langevin equation: non-Gaussian viscoelastic anomalous diffusion." *New Journal of Physics* 20, no. 2 (2018): 023026.
- [105] Sposini, Vittoria, Aleksei V. Chechkin, Flavio Seno, Gianni Pagnini, and Ralf Metzler. "Random diffusivity from stochastic equations: comparison of two models for Brownian yet non-Gaussian diffusion." *New Journal of Physics* 20, no. 4 (2018): 043044.
- [106] Lanoiselee, Yann, and Denis S. Grebenkov. "A model of non-Gaussian diffusion in heterogeneous media." *Journal of Physics A: Mathematical and Theoretical* 51, no. 14 (2018): 145602.
- [107] Lanoiselee, Yann, and Denis S. Grebenkov. "Non-Gaussian diffusion of mixed origins." *Journal of Physics A: Mathematical and Theoretical* 52, no. 30 (2019): 304001.
- [108] Slezak, Jakub, Krzysztof Burnecki, and Ralf Metzler. "Random coefficient autoregressive processes describe Brownian yet non-Gaussian diffusion in heterogeneous systems." *New Journal of Physics* 21, no. 7 (2019): 073056.
- [109] Metzler, Ralf. "Superstatistics and non-Gaussian diffusion." *The European Physical Journal Special Topics* 229, no. 5 (2020): 711-728.
- [110] Eliazar, Iddo I., and Igor M. Sokolov. "Measuring statistical evenness: A panoramic overview." *Physica A: Statistical Mechanics and its Applications* 391, no. 4 (2012): 1323-1353.
- [111] Eliazar, Iddo. "Harnessing inequality." *Physics Reports* 649 (2016): 1-29.
- [112] Eliazar, Iddo. "A tour of inequality." *Annals of Physics* 389 (2018): 306-332.

- [113] P.B. Coulter, *Measuring inequality: A methodological handbook* (Westview Press, Boulder, 1989).
- [114] G. Betti and A. Lemmi (Eds.), *Advances on income inequality and concentration measures* (Routledge, New-York, 2008).
- [115] L. Hao and D.Q. Naiman, *Assessing Inequality* (Sage, Los Angeles, 2010).
- [116] F. Cowell, *Measuring inequality* (Oxford University Press, Oxford, 2011).
- [117] Eliazar, Iddo. "Investigating equality: The Renyi spectrum." *Physica A: Statistical Mechanics and its Applications* 481 (2017): 90-118.
- [118] Kullback, Solomon, and Richard A. Leibler. "On information and sufficiency." *The annals of mathematical statistics* 22, no. 1 (1951): 79-86.
- [119] Kullback, Solomon. *Information theory and statistics*. Dover Publications (new edition) 1997.
- [120] Kessler, David A., and Eli Barkai. "Infinite covariant density for diffusion in logarithmic potentials and optical lattices." *Physical review letters* 105, no. 12 (2010): 120602.
- [121] Dechant, A., E. Lutz, E. Barkai, and D. A. Kessler. "Solution of the Fokker-Planck equation with a logarithmic potential." *Journal of Statistical Physics* 145, no. 6 (2011): 1524-1545.
- [122] Hirschberg, Ori, David Mukamel, and Gunter M. Schutz. "Approach to equilibrium of diffusion in a logarithmic potential." *Physical Review E* 84, no. 4 (2011): 041111.
- [123] Hirschberg, Ori, David Mukamel, and Gunter M. Schutz. "Diffusion in a logarithmic potential: scaling and selection in the approach to equilibrium." *Journal of Statistical Mechanics: Theory and Experiment* 2012, no. 02 (2012): P02001.
- [124] Barkai, E., E. Aghion, and D. A. Kessler. "From the area under the Bessel excursion to anomalous diffusion of cold atoms." *Physical Review X* 4, no. 2 (2014): 021036.
- [125] Ryabov, Artem, Ekaterina Berestneva, and Viktor Holubec. "Brownian motion in time-dependent logarithmic potential: exact results for dynamics and first-passage properties." *Journal of chemical physics* 143, no. 11 (2015): 114117.
- [126] De Santo, Serena, Pablo Villegas, Raffael la Burioni, and Miguel A. Munoz. "Simple unified view of branching process statistics: Random walks in balanced logarithmic potentials." *Physical Review E* 95, no. 3 (2017): 032115.

- [127] Ray, Somrita, and Shlomi Reuveni. "Diffusion with resetting in a logarithmic potential." *Journal of chemical physics* 152 (2020): 234110.
- [128] Onofri, Manuele, Gaia Pozzoli, Mattia Radice, and Roberto Artuso. "Exploring the Gillis model: a discrete approach to diffusion in logarithmic potentials." *Journal of Statistical Mechanics: Theory and Experiment* 2020, no. 11 (2020): 113201.
- [129] Paraguassu, Pedro V., and Welles AM Morgado. "The heat distribution in a logarithm potential." *Journal of Statistical Mechanics: Theory and Experiment* 2021, no. 2 (2021): 023205.
- [130] Pitman, James W. "One-dimensional Brownian motion and the three-dimensional Bessel process." *Advances in Applied Probability* 7, no. 3 (1975): 511-526.
- [131] De Long, David M. "Crossing probabilities for a square root boundary by a Bessel process." *Communications in Statistics-Theory and Methods* 10, no. 21 (1981): 2197-2213.
- [132] Imhof, J-P. "Density factorizations for Brownian motion, meander and the three-dimensional Bessel process, and applications." *Journal of Applied Probability* 21, no. 3 (1984): 500-510.
- [133] Cherny, A. S. "On the strong and weak solutions of stochastic differential equations governing Bessel processes." *Stochastics: An International Journal of Probability and Stochastic Processes* 70, no. 3-4 (2000): 213-219.
- [134] Katori, Makoto. *Bessel processes, Schramm-Loewner evolution, and the Dyson model*. Heidelberg: Springer, 2016.
- [135] N. H. Bingham, C. M. Goldie, and J.L. Teugels, *Regular variation* (Cambridge University Press, Cambridge, 1987).